4-2019

An investigation of the role of Ttyh1 in neuronal development via CRISPR/Cas9 genetic knockouts in Xenopus Laevis

Sabrina Bracero

An investigation of the role of Ttyh1 in neuronal development via CRISPR/Cas9 genetic knockouts in *Xenopus Laevis*

A thesis submitted in partial fulfillment of the requirement

for the degree of Bachelor of Science in Biology from

The College of William and Mary

by

Sabrina Esmeralda Bracero

Accepted for HONORS

Margaret S. Saha, Ph.D., Director

Jennifer Bestman, Ph.D.

Paul Heideman, Ph.D.

Robin Looft-Wilson, PhD.

Williamsburg, VA

May 3, 2019

Acknowledgements

First I would like thank my adviser, Dr. Saha, for all of her incredible mentorship. Throughout my three and a half years in the lab she has provided so much encouragement and countless opportunities that have helped me develop as a researcher. Her enthusiasm towards scientific research is truly inspiring and I cannot thank her enough for her constant support.

I would like to thank Sudip Paudel, Lauren Yi, and Charith Ratnayake for their amazing mentorship. They all spent countless hours working alongside me in lab, walking me through protocols, and helping me troubleshoot the many frustrations of my project.

I would also like to thank Nana Amoh and Rithvik Nalamalapu for their moral support through the writing process and the many late nights trying to make sense of data.

I would also like to Dr. Mark Forsyth for his generosity in the many time I urgently needed a reagent.

Of course, I must thank my family and friends who have always supported me and my pursuit of research. They have encouraged me in times where I was unsure and were always willing to listen or read anything I sent them.

Thank you also to my committee Dr. Bestman, Dr. Heideman, Dr. Looft-Wilson for their questions that made me think about my project a little deeper.

Table of Contents

List of Figures

List of tables

Abstract

Neural development is a highly regulated process that requires coordinated signaling in order to develop a properly functioning nervous system. One of these key signaling pathways is the Notch pathway, a highly conserved signaling pathway that plays a key role in development, particularly neural development. Recent studies have linked Ttyh1, a volume-sensitive chloride channel with a calcium-binding site, to the Notch signaling pathway. However, despite its importance in development and disease, Ttyh1 remains poorly studied. Previous work in the lab has shown that *Ttyh1* is highly expressed in the adult and developing nervous system, expression that has implications for the maintenance of neural stem cells and numerous cellular functions, such as cell communication, adhesion, and migration. This thesis project investigated the role of *Ttyh1* in neuro-development by genetically knocking it out using CRISPR/Cas9 genomic editing technology and investigating the expression of neural marker genes and the other members of the tweety family. Chromogenic *in situ* hybridization revealed knockout of *Ttyh1* resulted in differential expression of *Sox2*, a progenitor cell marker, and *tubb2b*, a differentiated neuronal marker. RT-qPCR analysis of *Ttyh1* knockouts did not result in a consistent significant difference in gene expression. These results suggest that Ttyh1 may be involved in neural stem cell development, but further investigation is needed to confirm its precise role.

Overview

Neural development requires highly coordinated regulation and signaling in order to successfully form the functioning nervous system. During embryonic development, the presumptive nervous system must differentiate and organize a multitude of neural cells including neurons, astrocytes, and oligodendrocytes (Kim et al., 2018). To accomplish such drastic rearrangement the developing embryo relies on highly conserved signaling processes governed by genes such as Sonic Hedgehog, Wnt, and Notch (Kim et al., 2018).

Notch specifically, is a highly conserved signaling pathway that can be found in all multicellular animals (Kopan et al., 2009). Notch signaling plays a key role in the development of almost all tissue types (Siebel et al., 2017). Some of the processes that Notch regulates include cell death, growth, migration, and determination of cell type (Kopan et al 2009; Bolos et al., 2007). Notch signaling functions over short distances, communicating between nearby cells through the release of signaling molecules binding to its receptors (Shimoji et al., 2011). Once signaling molecules bind and activate the receptors, Notch releases a subunit, which binds to DNA and results in a change in gene expression that maintains stem cell characteristics (Shimojo et al. 2011).

Recent studies have shown a link between Notch signaling and Ttyh1, a highly conserved volume sensitive chloride channel expressed in the nervous system (Kim et al., 2018). *Ttyh1* is a relatively newly discovered gene and not much is known about how it fits into molecular pathways (Campbell et al., 2000). However, Ttyh1 does have numerous implications in important cellular pathways, such as the cell communication, migration, structure, and maintenance of stem cell populations (Kim et al., 2018; Mathews et al., 2007; Jung et al., 2017;

Stefaniuk et al., 2010a). Ttyh1 has also been implicated in a number of diseases such as cancer, epilepsy, and brain damage (Matthews et al., 2007; Jung et al., 2017; Stefanuik et al., 2010b, Wiernasz et al., 2014).

The goal of this thesis was to investigate the role of the *Ttyh1* gene in neurodevelopment. Using CRISPR/Cas9 genetic editing technology, *Ttyh1* was specifically targeted and knocked out in *Xenopus laevis* embryos. Gene expression of key neural marker genes and other potential partners in *TTyh1* function were analyzed in *Ttyh1* knockout embryos via *in situ* hybridization and quantitative polymerase chain reaction.

Introduction

Notch Signaling

The Notch signaling pathway is a highly conserved pathway found in all metazoans, which has key functions in the development of most organs and tissues (Kopan et al., 2009; Siebel et al., 2017). Notch signaling has been found to participate in a variety of cellular processes including cell proliferation, apoptosis, differentiation, specification, adhesion, migration and maintenance of stem cell and progenitor cell populations throughout development and in self-renewing adult tissues (Kopan et al., 2009; Bolos et al ., 2007).

Notch signaling is activated by ligand binding to the Notch transmembrane protein (Shimoji et al., 2011). Once activated, the receptor undergoes proteolysis, releasing the active fragment of Notch, the Notch Intracellular domain (NICD) (Kopan et al., 2009; Shimojo et al., 2011). Following proteolysis, the NICD is imported into the nucleus where it forms a complex able to bind DNA and induce the expression of transcriptional repressors that then inhibit

differentiation and maintain neural stem cells and progenitor cells (Shimojo et al., 2011). Notch signaling typically acts over a short range and requires physical contact between cells (Kopan et al., 2009; Shimojo et al., 2011). Thus, cells inhibit differentiation of their neighbors through lateral inhibition (Shimojo et al ., 2011).

The involvement of Notch signaling in numerous cell processes also means that aberrant signaling is linked to multiple human disease. Developmental disorders include Alagille syndrome, tetralogy of Fallot, syndactyly, sonondylocostal dysotosis and familial aortic valve disease (Penton et al., 2012; Kopan et al., 2009). Notch signaling also has been implicated in cerebral autosomal dominant arteriopathy with subcortical infarcts and leukoencephalopathy (CADASIL) as well as cancer. Notch has also become the target for therapeutics for T cell acute lymphoblastic leukemia and colon cancer (Takebe et al., 2014).

Because Notch signaling is an ancient and highly conserved signaling pathway, and plays key roles in development, homeostasis, and disease, there is significant interest in understanding all of the major players in the Notch pathway as well as the effects of perturbation of the Notch pathway during embryonic development. Towards this end previous studies conducted in the lab performed a series of experiments that overexpressed and inhibited Notch signaling. Surprisingly, while perturbed embryos showed significant morphological deformities and aberrant gene expression early in development, by later stages the embryos appeared to compensate and showed few if any indications of the abnormalities. Early in development, the overexpression of Notch via injection of a synthetic intracellular domain (ICD) mRNA construct resulted in decreased expression of differentiated marker genes, increase in neural cell counts, slower neural tube closure, and a greater proportion of apoptotic

cells in *Xenopus laevis* embryos (Pownall et al., unpublished). On the other hand, inhibition of Notch signaling via injection of a DNA binding mutant (DBM) that blocks NICD's ability to act as a transcription factor, increased expression of differentiation marker genes. However, in both cases embryos displayed high levels of plasticity and were able to recover from the perturbations as development progressed. Based on these intriguing results, we performed RNA-seq analysis of perturbed embryos. While an entire suite of genes was differentially expressed, one of the genes in this list was particularly fascinating. A gene called, *Ttyh1* (Tweety) revealed a four-fold increase of expression following upregulation of the Notch signaling pathway. This suggested that the *Ttyh1* gene was involved in the Notch signaling pathway. Another study also linking*Ttyh1* to the Notch pathway showed that increased expression of *Ttyh1* resulted in increased expression of downstream genes in the Notch signaling pathway (Kim et al., 2018).

Tweety Homolog 1 (Ttyh1)

Ttyh1 is a member of the tweety gene family. The *Tweety* (Ttyh1) gene was first discovered in *Drosophila melanogaster* as a transcriptional unit with an unknown function adjacent to the flightless I gene (Campbell et al., 1993). *Tweety* has a broad phylogenetic distribution with orthologs existing in vertebrates, insects, slime molds, and plants (Matthews et al., 2007). In vertebrates the *tweety gene* family consist of three members, tweety homeolog 1 (*Ttyh1*), tweety homeolog 2 (*Ttyh2)*, and tweety homeolog 3 (*Ttyh3*) (Matthews et al., 2007). All three members of the tweety family have been characterized as large conductance chloride channels, maxi-Cl^-, with five transmembrane domains (Shizuki et al., 2004). *Ttyh2* and *Ttyh3*

encode Ca^{2+}-activated channels, whereas *Ttyh1* encodes a Ca^{2+}-independent, volume- sensitive Cl^- channel that is capable of binding Ca^{2+} (Suzuki et al., 2004; Kamada et al., 2010).

Ttyh1 is primarily expressed in the brain, eye, spinal cord, and testis, with lower levels expressed in the pancreas, pituitary gland, mammary gland, and liver (Matthews et al., 2007). During embryogenesis, *Ttyh1* is primarily expressed in the developing nervous system, with expression in the brain, spinal cord, eyes, and cranial ganglia as embryos continue to progress through neurogenesis (Halleran et al., 2015). In addition, *Tthy1* is expressed in stem cells and progenitor cells in proliferative, ventricular zones and subventricular zones (Halleran et al., 2015, Kumada et al., 2010). In adults, *Ttyh1* is abundant in terminally differentiated neural cells (Kumada et al., 2010). On a cellular level, *Ttyh1* has been found on the endoplasmic reticulum, Golgi apparatus, and clathrin coated vesicles in neurons and astrocytes, late endosomes or lysosomes of astrocytes, and axons and dendritic spines of neurons (Kumada et al., 2010, Weirnasz et al., 2014; Matthews et al., 2007; Stefanuik et al., 2010a).

Ttyh1 has been implicated in numerous cellular pathways and processes. Induced expression of *Ttyh1* in the embryonic kidney cell line, HEK293, resulted in high expression at cell-cell interfaces, an association with integrins, and cytoskeletal rearrangements suggesting a role in cell to cell communication, migration, and adhesion (Matthews et al., 2007). *Ttyh1* has also been associated with tumor microtubules in glioma cell proliferation, supporting its roles in cell migration and proliferation (Jung et al., 2017). Manipulation of *Ttyh1* expression also resulted in morphological changes in neurons *in vitro* (Stefaniuk et al.,2010a). In addition, *Ttyh1* has been shown to be critical for neural development in mice as homogeneous inhibition of the gene resulted in embryonic lethality prior to neural development (Kumada et al., 2010).

Induction of *Ttyh1* in primary mouse cell culture has been shown to support stem cell capacity (Kim et al., 2018). Additionally, *Ttyh1* is speculated to regulate ER Ca^{2+}, due to its ability to bind Ca^{2+} and its positioning in the lumen of the ER, and be involved in cell division, as it is highly expressed during the metaphase of mitosis (Kumada et al., 2010).

Ttyh1 has also been observed in numerous pathologies. Upregulation of *Ttyh1* has been observed in several forms of cancers, including astrocytoma and glioma, during epileptogenesis and epilepsy, and following brain damage in astrocytes (Matthews et al., 2007; Jung et al., 2017; Stefaniuk et al., 2010b; Wiernasz et al., 2014). Lower expression of *Ttyh1* has also been observed in breast cancer (Darweesh et al., 2014). In addition, the fusion of *Ttyh1* to a microRNA cluster have been shown to drive expression of the microRNAs in embryonal tumors with multilayered rosettes, a deadly form of pediatric brain tumor (Kleinman et al., 2014).

Because *Ttyh1* has clear links to the Notch signaling pathway, has robust expression in neural regions during early stages of development, is implicated in multiple cellular processes for neuron development, and is involved in numerous brain pathologies, *Ttyh1* is an excellent candidate for investigation. Moreover, despite its importance and clear clinical relevance, there have been relatively few studies of the gene, particularly functional investigations. The goal of this thesis was to investigate the role of *Ttyh1* in neurodevelopment by developing a protocol for CRISPR/Cas9 genomic knockouts in *Xenopus laevis* and investigating subsequent expression of neural marker genes, *Sox2* and *tubb2b*, the other members of the tweety family, *Ttyh2* and *Ttyh3*, and one of the Notch Receptors, *Notch1*. This project was conducted in *Xenopus laevis* because of its well characterized neural development, relatively fast development, and access to early stages of development.

Materials and Methods

Animal care

All animal care and procedures were performed in accordance with the College of William and Mary's Institutional Animal Care and Use Committee (IACUC) regulations. *Xenopus laevis* embryos were obtained through natural matings as described in Sive et al. (2000). Staging was done in accordance with Nieuwkoop and Faber (Nieuwkoop and Faber, 1994).

CRISPR guide RNA design and synthesis

Guide RNA (gRNA) for CRISPR/Cas9 mutagenesis was designed using Harvard's CHOP CHOP site (http://chopchop.cbu.uib.no/). The site evaluates the gene of interest FASTA sequence for potential target sites based on GC content, off target sites, and self-complementarity. The gRNA was selected based on ranking, location in the sequence, and termination with the *S. pyogenes* Cas9 protospacer adjacent motif (PAM) site, NGG. The gRNA sequence was then confirmed in the gene of interest via BLAST. The final gRNA sequence selected was: GGAATTGGCATTGGTTTCTA**CGG**, with the PAM site in bold. An oligo was then designed with the gRNA without the PAM site, the promoter site for SP6 polymerase (lowercase), and an overlap region for the constant region (lowercase and bold). The final oligo sequence ordered was:

atttaggtgacactataGGAATTGGCATTGGTTTCTA**gttttagagctagaaatagcaag**. The oligonucleotide for the constant region ordered was:

AAAAGCACCGACTCGGTGCCACTTTTTCAAGTTGATAACGGACTAGCCTTATTTTAACTTGCTATTTCTAG

CTCTAAAAC. All oligonucleotides were ordered from Integrated DNA technologies (IDT). 100 µM of both oligonucleotides were hybridized in duplexing buffer (10mM Tris, 1 mM EDTA, 50mM NaCL) for 5 min at 95 C, then cooled for 1hr at room temperature (RT). Approximately 2uM of annealed oligonucleotide solution was then was filled in via polymerase chain reaction (PCR) using Q5 Hot Start 2x master mix from New England Biolabs (NEB), with the following reaction 94 C for 5 min, 20 cycles of 94 C 20 sec, 58 C 20 sec, 68 C 15 sec, 5 min 68 C. The complete oligonucleotide was then cleaned up using NEB PCR clean up kit according to the manufacturer's instructions. The uncapped gRNA was transcribed using the mMessage mMachine kit according to manufacture instructions and purified using Qiagen RNeasy Mini Elute Cleanup kit according to manufacturer's instructions. Purified gRNA was stored in -80 until injected.

Injections and screening

Cas9 protein was ordered from IDT and stored at -20. Cas9 was combined with purified gRNA and allowed to incubate at RT for 10 min. The cas9/gRNA solution was then diluted with 5% Fluoresceinated lysine-fixable dextran (FLDX). Embryos were injected bilaterally at the 2-cell stage with 9.2 nL of the construct. For the FULL concentration embryos received 2.3 ng of gRNA and 5.2ng of Cas9. For the HALF concentration embryos received 1.15 ng of gRNA and 2.6 ng of Cas9. For FLDX controls embryos were injected with diluted FLDX for a total 0.6 µg of FLDX. Non-injected controls were also selected. Embryos were also injected unilaterally at the 2-cell stage receiving 1.15 ng of gRNA and 2.3 ng of Cas9. Embryos were injected in a 1/3 Marc's Modified Ringers (MMR) and 4% Ficoll, from Sigma, solution. Embryos were allowed to recover

in 1/3 MMR and 4% ficoll at 16 C. 1.5-2 hrs following injections necrotic embryos were removed and healthy embryos were moved to a 0.1X MMR and 4% ficoll solution and remained at 16 C. Necrotic embryos were removed and solution was changed 6 hrs and 9 hrs post injection, then allowed to recover overnight at 16 C. Injected embryos were either tracked for mortality every 3-4hrs or grown to NF stages 20, 30, or 40 for nitrogen or MEMFA fixation (method described below). Mortality tracked embryos received a solution change every 3-4 hrs of 0.1xMMR and 4% ficoll until completion of gastrulation where the solution was changed to 0.1x MMR and Gentamycin. Following NF stage 20 mortality tracked embryos received solution changes only twice a day with 0.1x MMR and Gentamycin. The solution was changed at each timepoint. Necrotic Embryos were also removed at each time point.

Fixation (MEMFA and Nitrogen)

Injected embryos for fixation were screened for fluorescence with a Nikon SMZ800N stereomicroscope. Unilaterally injected embryos were also screened for left or right injection at stage 20 or 30. Embryos for *in situ hybridization* were fixed in MEMFA (100 mM MOPS, pH 7.4, 2 mM EGTA, 1 mM MgSO4, 4% Formaldehyde), washed in 100% ethanol and stored at -20 C. Embryos for DNA and RNA extraction were individually flash frozen in liquid nitrogen and stored at -80 C.

Whole Mount In Situ Hybridization

Antisense probes for neural marker genes *tubb2* (Klein et al., 2002) and *Sox2* (Huyck et al., 2015) were synthesized with digoxigenin-substituted uracil nucleotides according to Sive et

al. (Sive et al., 2000). Spatial expression of the genes was analyzed via chromogenic *in situ* hybridization as described in Sive et al. with minor modifications, using NBT/BCIP (nitrobluetetrazolium/5-bromo-4-chloro-3-indolyl phosphate) alkaline phosphatase substrates (Sive et al., 2000). Whole mount images were taken in phosphate buffer saline on a Nikon SMZ800N stereomicroscope attached to a Nikon DS-Ri2 camera.

Histology

For histological analysis, embryos were dehydrated in 100% ethanol followed by dehydration in 100% xylene and embedded and set in 100% paraffin for a minimum of 18 hours. Embryos were sectioned into 18 µm-thick transverse slices on a microtome, mounted onto glass slides, and cover slipped with permount. Sections were photographed using an Olympus BX60 scope attached to an AmScope MU1400 digital camera. Histological structures were determined based on Hausen et al. (1991).

DNA and RNA extractions

Genomic DNA and RNA were extracted from nitrogen fixed embryos using TRI reagent by Thermo Fisher. Embryos were individually homogenized in 100 µl of Tri Reagent. RNA was isolated using 20 µl of chloroform. The aqueous phase was collected, and RNA was precipitated out with 50 µl Isopropanol. The RNA pellet was then washed in 75% ethanol, allowed to dry, and resuspended in 30µl of nuclease free water. Genomic DNA was precipitated out of the interphase layer using 100% Ethanol, then washed with 70% ethanol, allowed to dry and resuspended in 20 µl of TE.

Reverse Transcription and Quantitative Polymerase Chain Reaction

Approximately 500ng of extracted RNA was reverse transcribed using iScript by BioRad according to the manufacturer's instructions. Gene expression was analyzed using TaqMan Universal qPCR Master Mix and StepOne Real-Time PCR according the manufacturer's instructions. Custom primers and probes were ordered and designed using the Custom TaqMan Gene Expression Assays. Cycling conditions were: 95 C 10 min; 40 cycles of 95 C 15 sec, 60 C 1 min. TaqMan probes were labeled at the 5' end with FAM dye and at the 3' end with the NFQ quencher. Primers used were: tubb2b, 5' - GGCAGATTTTCAGACCAGACAACTT – 3' and 5' - GACCTTTGGCCCAGTTATTGC- 3'; Notch1, 5' - CAAGCAGGACATTAATGAGTGCAG-3' 5-AGCGGTATGATCCAAACTCATTGAT-3'; ttyh2, 5'-CTGGACTGCTGCTGTGTCT and 5'-CATTGGTCTCACTGTTCCCATAGAA-3'; ttyh3, 5'-TGGAAGAATCATTACTTGCTGGATGAA-3' and 5'-CAGAAGCAGGCCCAGGTA-3'; Drosha, 5'-ACCCCGATCGCCTTCATG-3' and 5'-GGCTTTCAAACTGCACTTACAGAGA-3'. The sequence for Sox2 primers was unavailable, but will be available once probe and primers are re-ordered. Raw data were processed with StepOne Software v2.3. Data was normalized to Drosha RNA (ΔΔCT analysis).

Polymerase Chain Reaction and Sequencing

Primers approximately 200 bp upstream of the target site were designed. Forward: 5'-GCAGGACAAAAGAAGAAAGCTGTA-3' and Reverse 5'-CTGGTTAGTGGGACAGAGCAG-3'. PCR was performed using NEB Q5 High Fidelity PCR Master mix according to manufacture's instructions using extracted genomic DNA. Cycling conditions were: 98 C 30 sec, 30 cycles of 98 C 10sec,

65 C 30sec 72 C 30 sec; 72 2 min; hold at 4 C. PCR products were purified using NEB PCR clean up kit according to manufactured instructions, then sequenced using sanger sequencing using the same primers for PCR.

TIDE: Tracking of Indels by Decomposition Analysis

CRISPR mutation efficiency was analyzed using the TIDE online tool (https://tide.deskgen.com/) developed by Brinkman et al., 2014. The gRNA sequence along with the chromatogram files from sequencing of a control sample and a test sample are submitted to the website. TIDE first aligns the gRNA sequence to the control sample to predict the cut site, then aligns the region upstream of the predicted cut site of the test and control sample. The software then analyzes the peak heights of the chromatograms for each base downstream of the cut site to determine the relative abundance of aberrant nucleotides in the sequence provided. TIDE creates sequence trace models of possible insertions and deletions (INDEL) based on the control sample. The program then runs a goodness of fit analysis of the test sample to a combination of control sample and the predicted INDELs. TIDE calculates the p-value for the abundance of a given INDEL in the population via two-tailed t-test of the variance–covariance matrix of the standard errors. The program then sums the abundance of statistically significant INDELs to provide a percent mutation efficiency, which is the percentage of the sequence population that contains an INDEL mutation.

All experimental samples were compared to a non-injected control of the same stage from the same injection date. One non-injected control sample was selected for comparison for each injection date and staged based on Xenbase BLAST identity percentage match to *Ttyh1*L.

Statistical Analysis

Statistical difference of the mean percent mutation efficiencies of experimental conditions was calculated using unpaired, unequal variance, two-tailed T-test in Excel. The standard deviation was also calculated in Excel.

Percent survival was calculated at the end of each mortality experiment by dividing the total living embryos by the initial number of embryos placed into the plate. The mean was taken across all three mortality experiments. The statistical difference of the mean survival rate between replicates was calculated using unpaired, unequal variance, two-tailed T-test in Excel. The standard deviation was also calculated in Excel.

qPCR ΔC_T values were calculated by subtracting the mean C_T values of technical replicates for the housekeeping gene, *Drosha*, from the mean C_T of the gene of interest. $\Delta\Delta C_T$ were calculated by subtracting the mean ΔC_T of the biological controls from the ΔC_T of each sample. $\Delta\Delta C_T$ were calculated using the mean ΔC_T for stage 20 and 30 separately and mean ΔC_T across both stages. The fold change was calculated by setting 2 to the power of the negative $\Delta\Delta C_T$ ($2^{-(\Delta\Delta CT)}$). Difference between experimental conditions was calculated using unpaired, unequal variance, two-tailed T-test in excel on the $2^{-(\Delta\Delta CT)}$ value for stage 20 and 30, separately and both stages combined. Linear regression analysis was calculated using the regression tool in the Data Analysis tool pack in Excel where TIDE mutation efficiency was the independent variable and the $2^{-(\Delta\Delta CT)}$ was the dependent variable. All calculations were done in Microsoft Excel.

Results

Mutation Efficiency

To determine the success of the CRISPR/Cas9 Knockout of*Ttyh1*, genomic DNA (gDNA) was extracted from individual embryos. PCR products of the target site were then sequenced and analyzed using the Tracking of Indels by Decomposition (TIDE) developed by Brinkman et al. (2014). TIDE analysis of stage 20 and 30 embryos injected with the higher concentration of 2.3 ng gRNA and 5.2 ng Cas9 (FULL) had an average mutation efficiency of 41.4%, with a high degree of variability (SD 37.7, n = 22) (**Figure 1A**). For embryos injected with 1.15 ng gRNA and 2.6 ng Cas9 (HALF) the average mutation efficiency was 26.7% (SD 33.66, n = 5), for FLDX injected controls (FLDX) the average was 5.08% (SD 3.55, n =6), and for non-injected controls (CON) the average was 0.17% (SD 0.44, n= 12). FULL embryos had a significantly higher mutation efficiency as compared to CON (p = 5e -5) and FLDX (p = 2.3e -4) embryos. There was not a significant difference in mutation efficiency between FULL and HALF embryos (p = 0.26). There was a significant difference between CON and FLDX embryos (p = 0.027) when mutation efficiency was analyzed in both stages together.

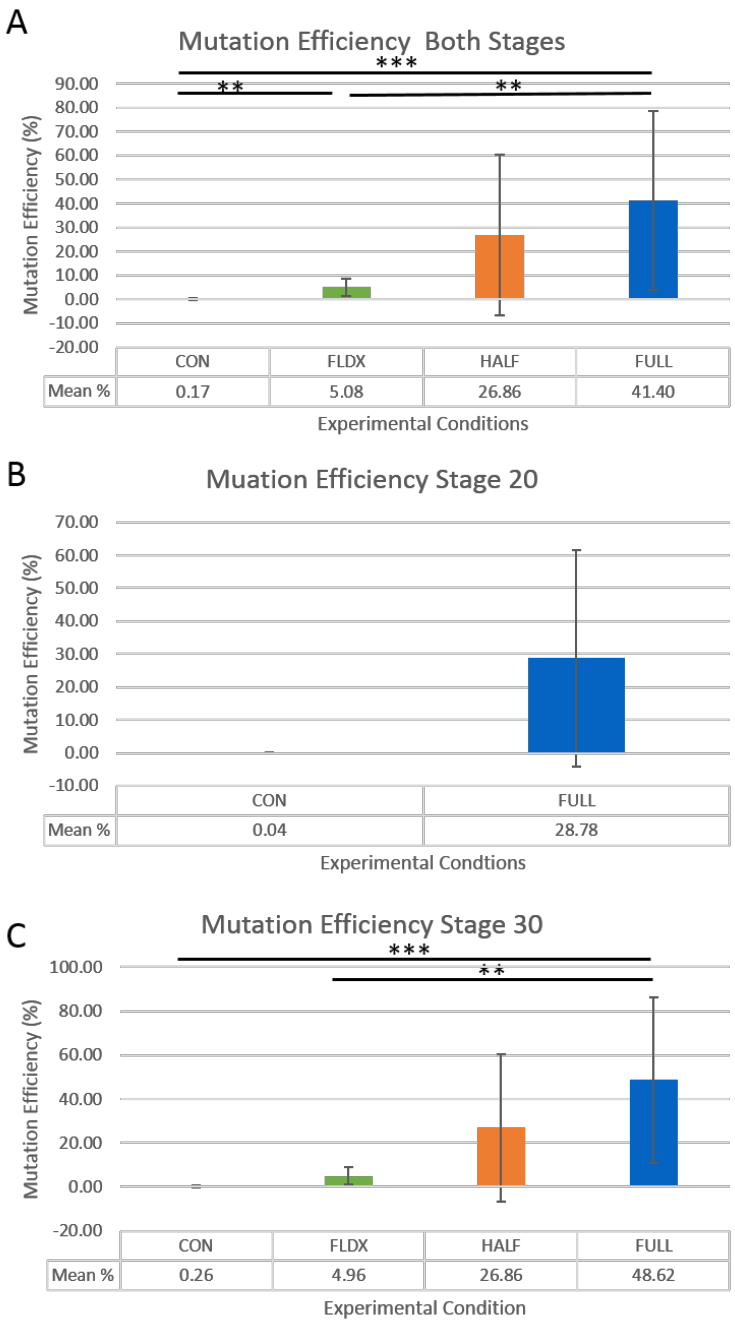

Figure 1. Mutation Efficiency of CRISPR/Cas9* Ttyh1 *Knockouts

(A-C) Average percent mutation efficiency of based on Tracking of Indels by Decomposition (TIDE). FULL (2.3ng gRNA, 5.2ng Cas9), HALF (1.15ng gRNA, 2.6ng Cas9), FLDX (5% Fluoresceinated lysine-fixable dextran) and Con (non-injected control) embryos. (A) TIDE analysis of mutation efficiency in NF stage 20 and 30 (FULL, n = 22), (HALF, n = 5), (FLDX, n = 6), (Con n = 12). (B) TIDE Analysis of mutation efficiency in NF stage 20 embryos (FULL, n = 8), (Con, n = 5), . (C) TIDE analysis of mutation efficiency in stage NF 30 (FULL, n = 14), (HALF, n = 5), (FLDX, n = 5), (Con n = 7). (** = $p \leq 0.01$; *** = $p \leq 0.001$), error bars indicate 1 standard deviation.

The mutation efficiency was also analyzed by stage. At stage 20 the average mutation efficiency was 28.78% (SD 32.88, n = 8) for FULL and 0.04% (SD 0.08, n = 5) for CON embryos (**Figure 1B**). The difference in mutation efficiency between FULL and CON embryos at stage 20 was just below the threshold of significance ($p = 0.054$). At stage 30 mutation efficiency was 48.62% (SD 37.66, n = 14) in FULL, 26.86% (SD 33.66, n =5) in HALF, 0.26% (SD 0.55, n = 7) in CON, and 4.96% (SD 3.88, n =5) in FLDX embryos (**Figure 1C**). Mutation efficiency was significantly higher in FULL embryos as compared to CON ($p = 5e\text{-}4$) and FLDX injected controls (FLDX) ($p = 0.0011$). The mutation efficiency was not significantly different between FULL and HALF embryos at stage 30 ($p = 0.31$). Together these data suggest that injection of the FULL concentration is able to successfully induce a mutation in *Ttyh1*.

Mortality

To determine if CRISPR/Cas9 Knockout of *Ttyh1* had significant effects on mortality, survival of embryos bilaterally injected with the full concentration 2.3 ng gRNA, 5.2 ng Cas9 (FULL), half concentration of 1.15 ng gRNA and 2.6 ng Cas9 (HALF), a control injection with just FLDX (FLDX), and non-injected controls (CON) were monitored (**Figure 2**). Figures2A-C depict

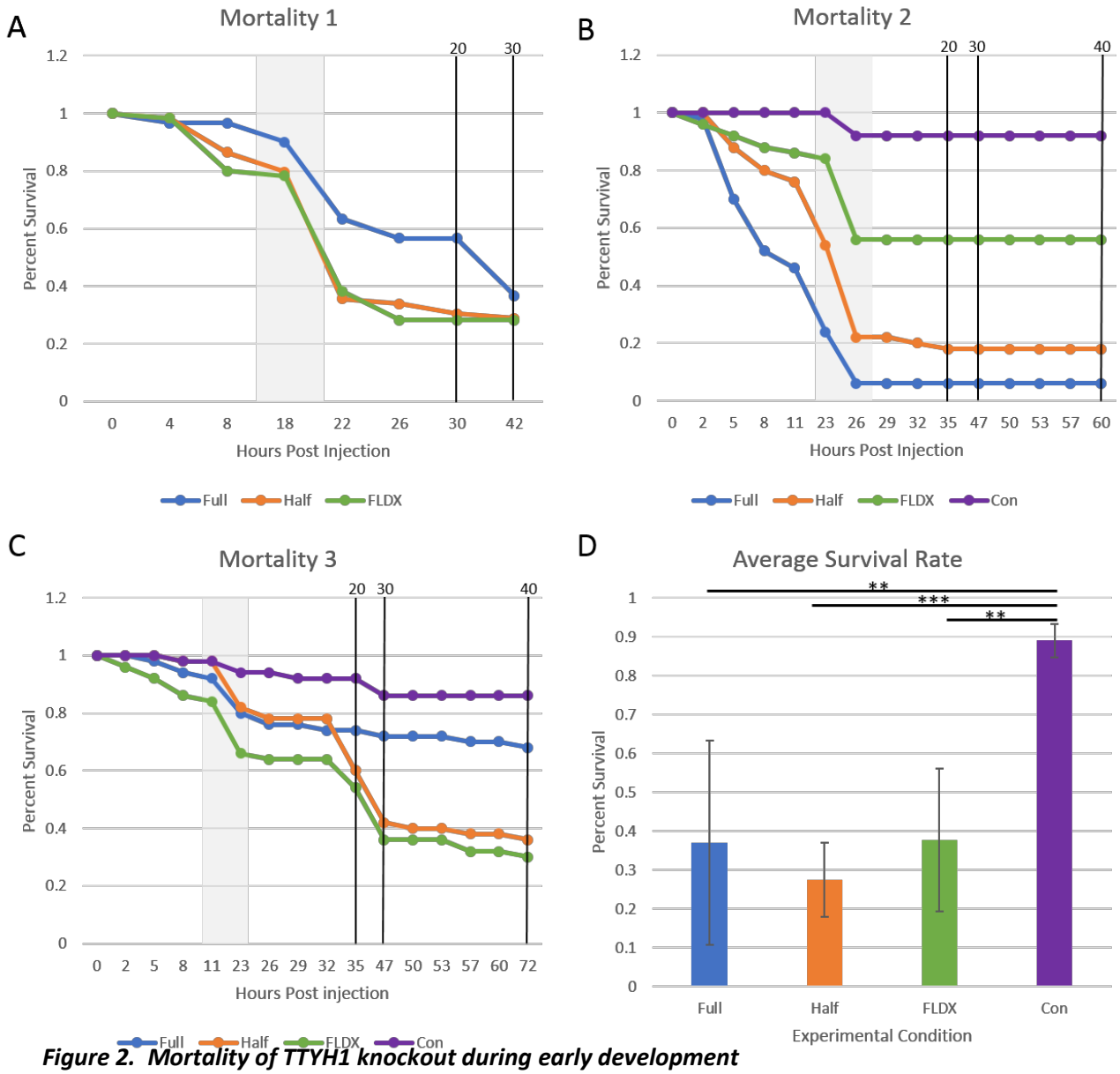

Figure 2. Mortality of TTYH1 knockout during early development

(A-C) Percent survival of bilaterally injected three independent replicates (Full 2.3ng gRNA, 5.2ng Cas9; Half 1.15ng gRNA, 2.6ng Cas9; FLDX 5% Fluoresceinated lysine-fixable dextran) and non-injected control (Con) embryos from injection (0hrs) to NF stage 30 (A) or NF st40 (B,C). (A) n = 30 in duplicate for all experimental conditions (B,C) n = 25 in duplicate for all experimental conditions. Gray background indicates gastrulation. Black vertical lines indicate NF stage (D) Average survival rate across mortality replicates (** = $p \leq 0.01$; *** = $p \leq 0.001$), error bars

the percent survival over the course of 2 or 3 days mortality was tracked. The first mortality experiment was only monitored until embryos reached NF stage 30 (**Figure 2A**), mortality 2

(**Figure 2B**) and 3 (**Figure 2C**) were monitored until embryos reached NF stage 40. The survival often declined in the first 12hrs following injections, during overnight incubations, or during gastrulation. Survival became relatively stable once embryos reached stage 30. FULL embryos had a high mortality rate, with an average survival rate of 37.01% (SD = 26.26). HALF embryos had an average survival rate of 27.53% (SD = 9.5). FLDX embryos had an average survival rate of 37.75% (SD = 18.29). In all replicates, CON embryos had the best and most consistent survival rate, with an average of 89.00% (SD = 4.36). On average, FULL embryos did not have survival rate that was statistically different from HALF embryos ($p = 0.47$) or FLDX embryos ($p = 0.95$). All injected embryos had significantly higher mortality rates as compared to control embryos: FULL ($p= 0.0062$), HALF ($p = 2.6e-6$), FLDX ($p = 0.0010$).

In Situ Hybridization of Bilaterally- and Unilaterally-injected Embryos

To determine the effects of*Ttyh1* knockouts on neurodevelopment, *in situ* hybridization was performed on bilaterally and unilaterally injected embryos to visualize *Sox2,* a transcription factor that is a marker for neural progenitor cells, and *tubb2b*, a neuron-specific microtubule component expressed in differentiated neurons (Graham et al., 2003; Moody et al., 2007). Bilaterally injected embryos appeared to have less expression of *Sox2* at NF stage 30 and 40 throughout the developing the nervous system (**Figure 3**). Differences in expression were most noticeable at NF stage 30 (**Figure 3A-D**). Bilateral embryos also appeared to have lighter expression of *tubb2b* at NF stages 30 and 40, throughout the developing nervous system (**Figure 4**).

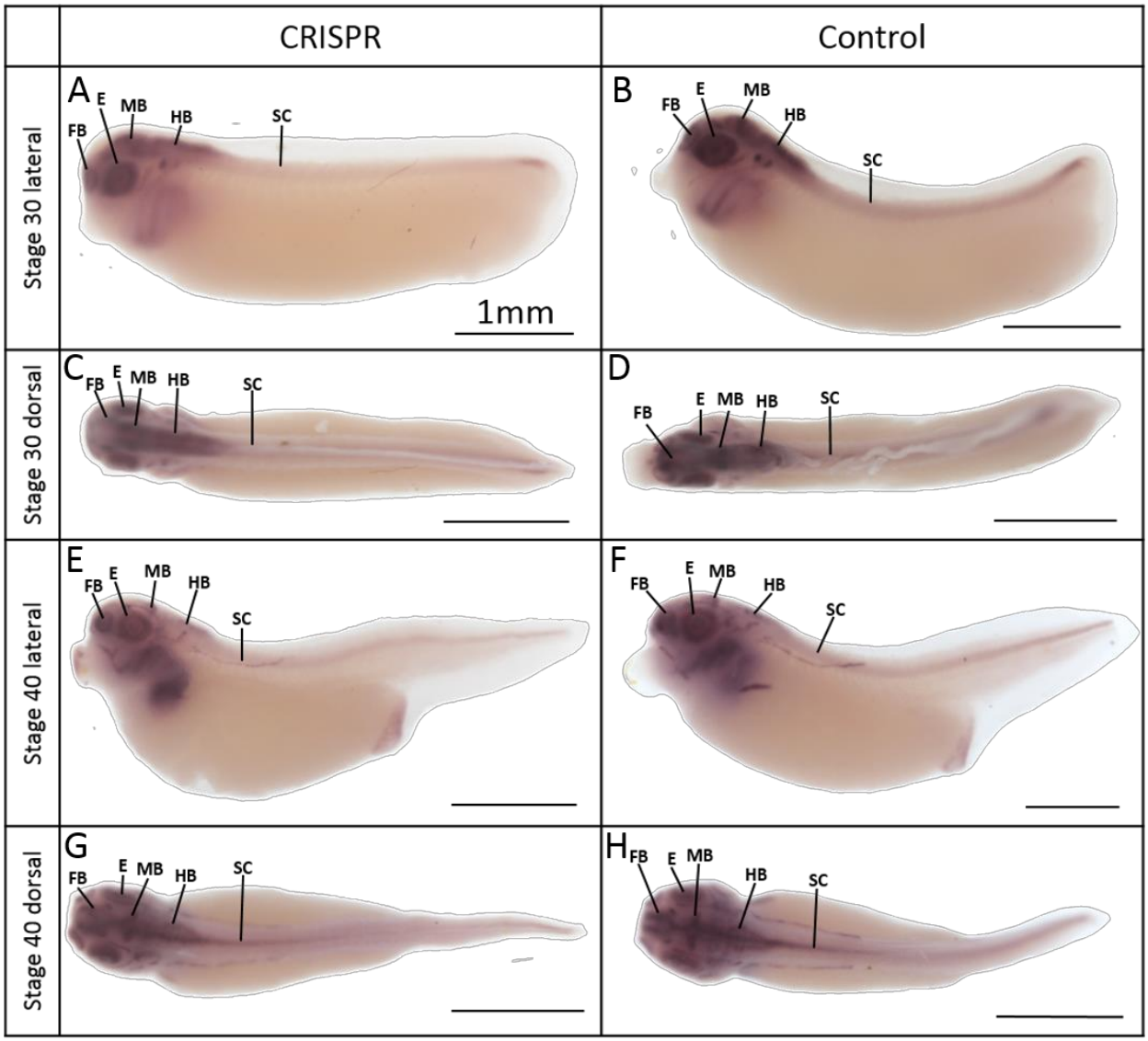

Figure 3. Expression of Sox2 in bilaterally injected embryos

Representative images of Sox2 expression in embryos bilaterally injected with 1.15ng TTYH1 gRNA and 2.6ng Cas9 and non-injected controls. (A,C) NF stage 30 bilaterally injected with CRISPR construct (A) lateral view, (C) dorsal view. (B,D) NF stage 30 non-injected control (B) lateral view, (D) dorsal view. (E,G) NF stage 30 bilaterally injected with CRISPR construct (E) lateral view, (G) dorsal view. (F,H) NF stage 30 non-injected control (F) lateral view, (H) dorsal view. Scale bar is 1mm in all images. N = 12 for all condition Abbreviations: I/M intermediate/medial longitudinal stripes of primary neurogenesis; FB, forebrain; E, eye; MB, midbrain; HB, hindbrain; SC, spinal cord.

Embryos were also injected unilaterally and analyzed for marker gene expression to compare the effects of*Ttyh1* knockdown within the same genetic background. Consistent with bilaterally injected embryos, Sox2 expression was less prominent on the injected side of the

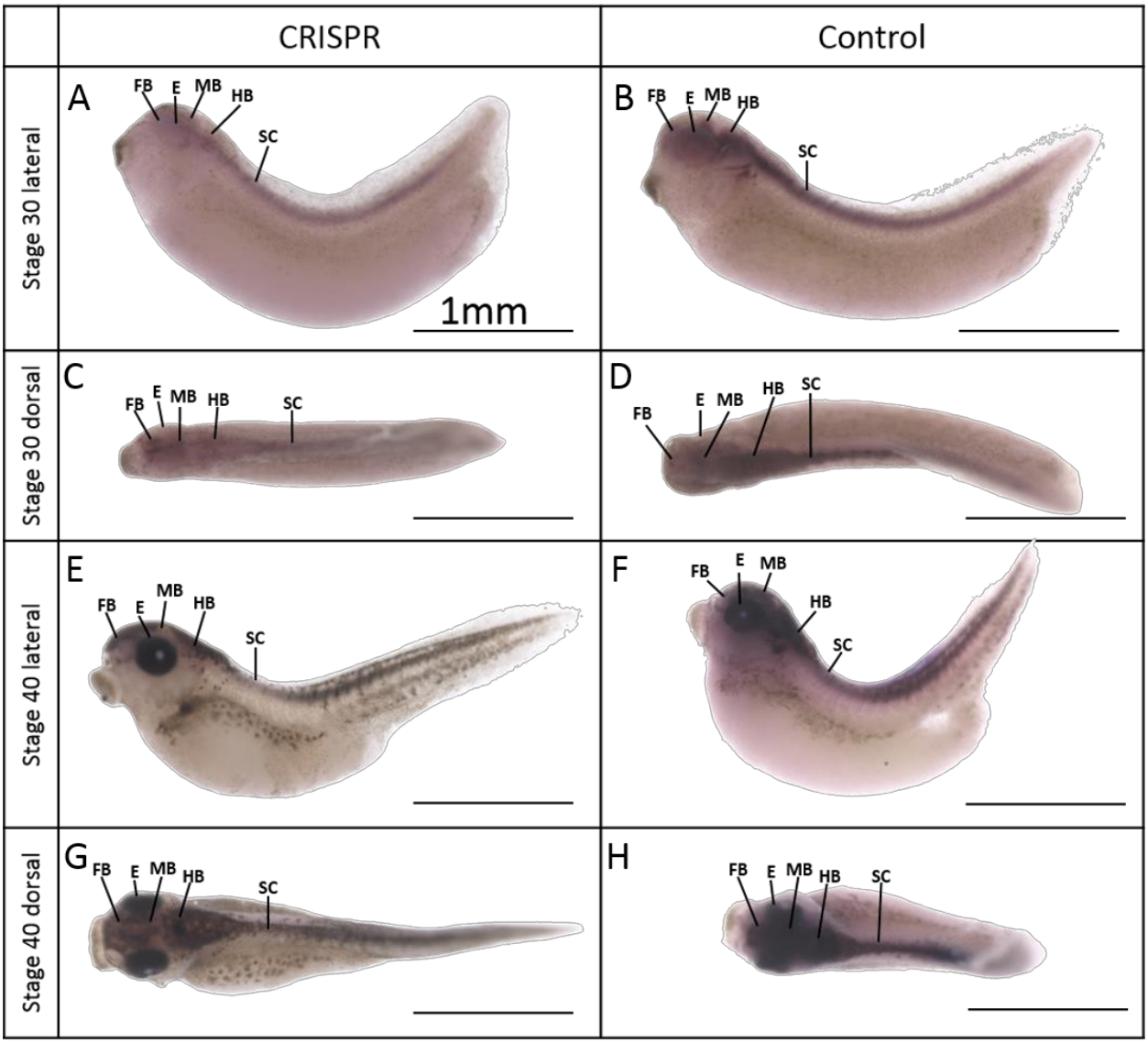

Figure 4. Expression of NBT in bilaterally injected embryos
Representative images of NBT expression in embryos bilaterally injected with 1.15ng TTYH1 gRNA and 2.6ng Cas9 and non-injected controls. (A,C) NF stage 30 bilaterally injected with CRISPR construct (A) lateral view, (C) dorsal view. (B,D) NF stage 30 non-injected control (B) lateral view, (D) dorsal view. (E,G) NF stage 30 bilaterally injected with CRISPR construct (E) lateral view, (G) dorsal view. (F,H) NF stage 30 non-injected control (F) lateral view, (H) dorsal view. Scale bar is 1mm in all images. N = 12 for all condition. Abbreviations: I/M intermediate/medial longitudinal stripes of primary neurogenesis; FB, forebrain; E, eye; MB, midbrain; HB, hindbrain; SC, spinal cord.

embryo, with the most apparent differences in NF stage 30 embryos (**Figure 5**). Expression of *tubb2b* in unilaterally injected embryos was more dynamic (**Figure 6)**. *Tubb2b* had more intense expression in the injected side in NF stage 20 embryos (**Figure 6A-C)**. By NF stage 30 *tubb2b*

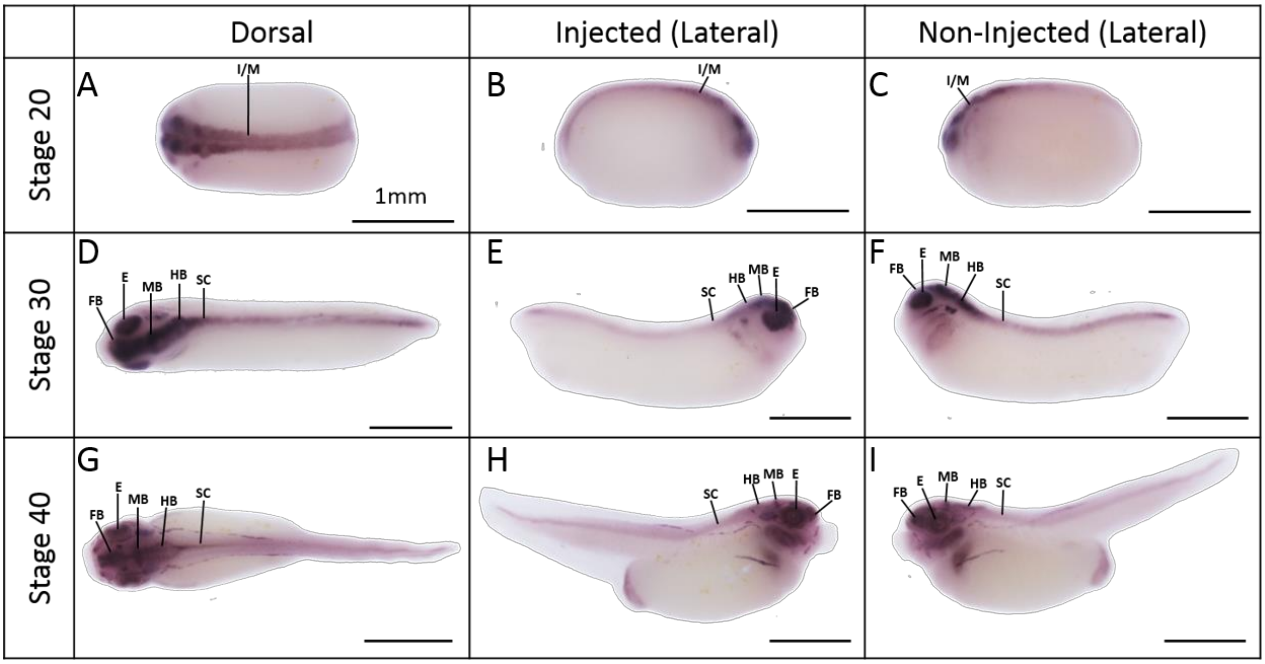

Figure 5. Expression of Sox2 in unilaterally injected embryos.
Representative images of Sox2 expression in embryos unilaterally injected with 1.15ng TTYH1 gRNA and 2.6ng Cas9. (A-C) NF stage 20 same embryo with views of dorsal (A) lateral injected side (B) and lateral non-injected side (C), (D-F) NF stage 30 same embryo with views of dorsal (D) lateral injected side (E) and lateral non-injected side (F). (G-I) NF stage 40 same embryo with views of dorsal (G) lateral injected side (H) and lateral non-injected side (I). (A, D, G) Dorsal view. Injected side is the lower half of the embryo in all three panels. Scale bar is 1mm in all images. N = 8 for all condition
Abbreviations: I/M intermediate/medial longitudinal stripes of primary neurogenesis; FB, forebrain; E, eye; MB, midbrain; HB, hindbrain; SC, spinal cord.

expression was visually the same on injected verse the non- injected side (**Figure 6D-F**). At NF stage 40 *tubb2b* expression was more intense in the non-injected side of the embryo (**Figure 6G-I)**, consistent with bilaterally injected embryos ay the same stage.

Histology of unilaterally injected embryos was performed to examine the spatial expression of marker genes following knockout of *Ttyh1* with greater resolution along both the anterior-posterior and dorsal-ventral axes. Expression of *Sox2* in histological sections was more prominent on the non-injected side, consistent with whole mount images (**Figure 7**). Differences in Sox2 expression were the most visually apparent at NF stage 30, with differences

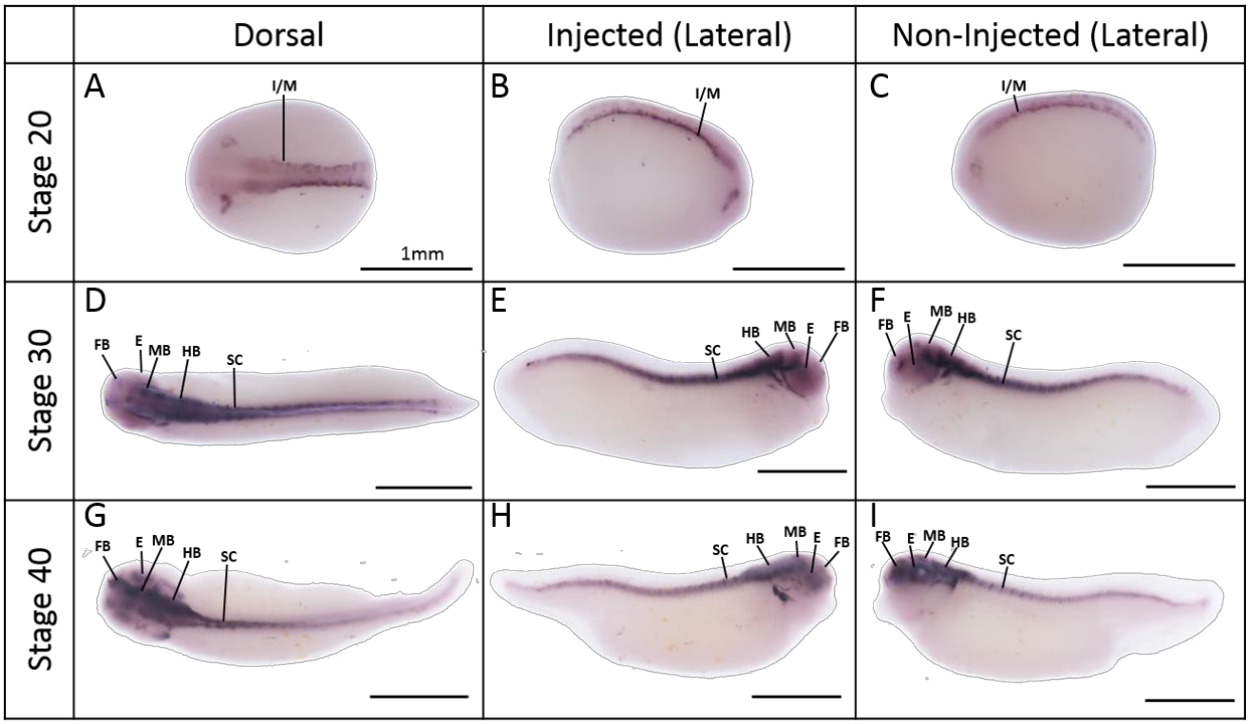

Figure 6. Expression of tubb2b in unilaterally injected embryos
Representative images of tubb2b expression in embryos unilaterally injected with 1.15ng TTYH1 gRNA and 2.6ng Cas9. (A-C) NF stage 20 same embryo with views of dorsal (A) lateral injected side (B) and lateral non-injected side (C), (D-F) NF stage 30 same embryo with views of dorsal (D) lateral injected side (E) and lateral non-injected side (F). (G-I) NF stage 40 same embryo with views of dorsal (G) lateral injected side (H) and lateral non-injected side (I). (A, D, G) Dorsal view. Injected side is the lower half of the embryo in all three panels. Scale bar is 1mm in all images. N = 8 for all condition Abbreviations: I/M intermediate/medial longitudinal stripes of primary neurogenesis; FB, forebrain; E, eye; MB, midbrain; HB, hindbrain; SC, spinal cord.

in expression noticeable throughout the entire anterior-posterior axis of the developing brain, neural crest, and spinal cord (**Figure 7G-L)**. Differences in expression for stages 20 and 40 were most apparent in the anterior sections of the embryo (**Figure 7A-B; 6N).**

Expression of *tubb2b* in histological sections was also consistent with whole mount images (**Figure 8**). At NF stage 20 *tubb2b* expression was more intense in the injected side throughout the neural crest along the entire anterior posterior axis (**Figure 8A-F**). At NF stage 30, hatching stages, *tubb2b* expression appeared darker in the non-injected side, which was more apparent in anterior sections in the neural crest (**Figure 8G,H**). However, expression in the

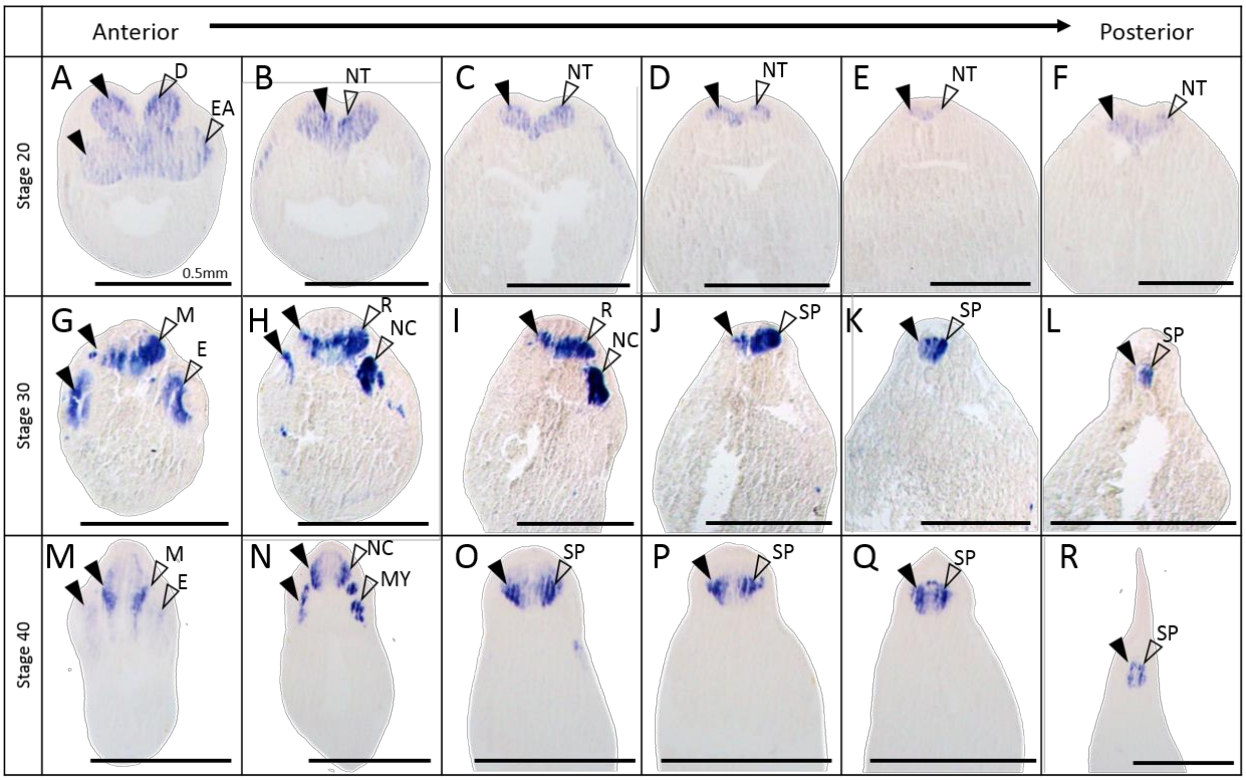

Figure 7. Expression of Sox2 in histological sections of unilaterally injected embryos
Representative images of embryos injected unilaterally with 1.15ng TTYH1 gRNA and 2.6ng Cas9. (A-F) NF stage 20 embryo sections anterior to posterior. (G-L) NF stage 20 embryo sections anterior to posterior. (M-R) NF stage 40 embryo sections anterior to posterior. N = 2 for all conditions Filled in arrows, expression on the injected side; hollow arrows, expression on the un-injected side. Injected side is on the left in all panels. D, deuterencephalon. EA, eye anlage. NT, neural tube. E, eye vesicle. M, mesencephalon. NC, neural crest. R, rhombencephalon. MY, Myotome. SP, Spinal Chord Scale bar is 0.5mm.

prosencephalon appeared more intense in the injected side **(Figure 8G).** At stage 40, *tubb2b* expression appeared darker in the non-injected side, which was more apparent in anterior sections in the prosencephalon, mesencephalon, eye regions, and otic vesicle (**Figure 8 M-O**).

Quantitate Polymerase Chain Reaction Gene Expression

Expression analysis of *Sox2* is summarized in **Table1** and **Figure 9**. The only significant difference in expression was between the two concentrations of CRISPR/Ca9 injected where

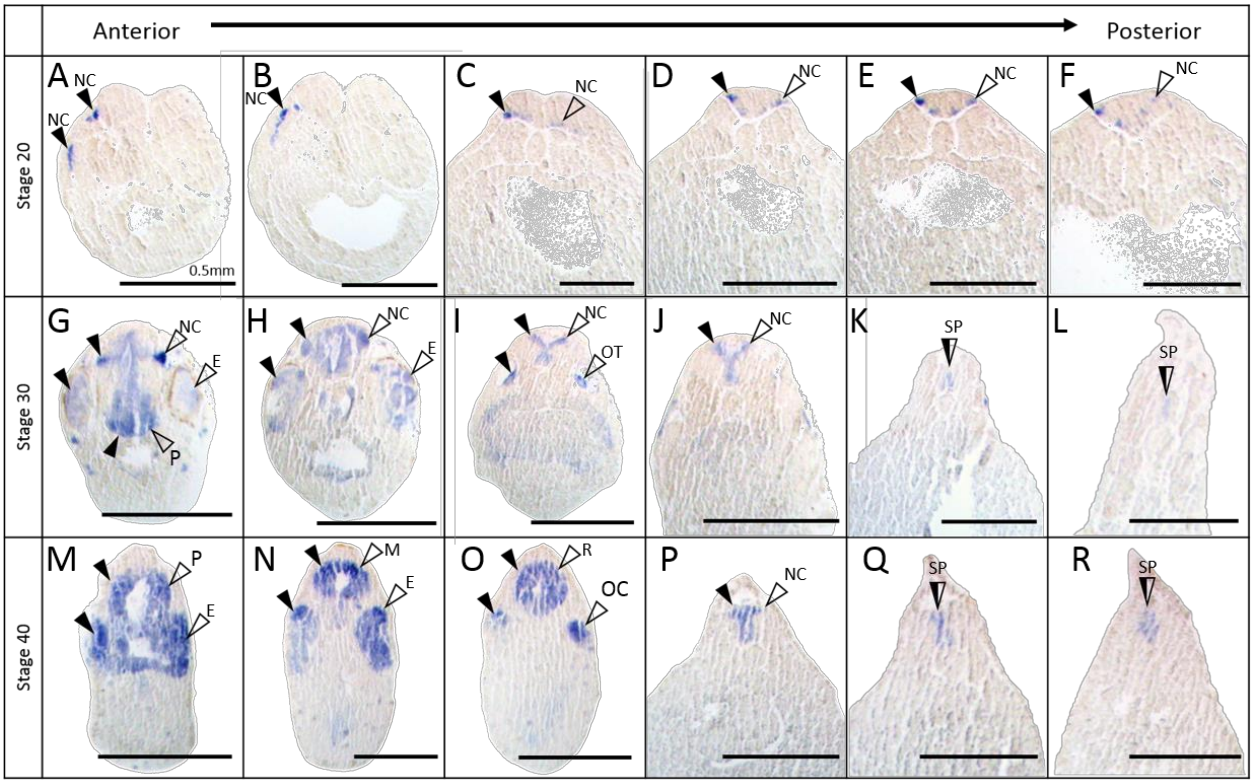

Figure 8. Expression of tubb2b in histological sections of unilaterally injected embryos
Representative images of embryos injected unilaterally with 1.15ng TTYH1 gRNA and 2.6ng Cas9. (A-F) NF stage 20 embryo sections anterior to posterior. (G-L) NF stage 20 embryo sections anterior to posterior. (M-R) NF stage 40 embryo sections anterior to posterior. N = 2 for all conditions Filled in arrows, expression on the injected side; hollow arrows, expression on the un-injected side. Injected side is on the left in all panels. (NC, neural crest; P, prosencephalon. E, eye. SP, Spinal Cord. M, mesencephalon. R, rhombencephalon OT, otic vesicle. OC, otocyst). Scale bar is 0.5mm.

FULL embryos had significantly higher expression of Sox2 as compared to HALF embryos (p = 0.04) (**Table 1**). At stage 30, difference in expression between HALF embryos and and non-injected controls was just above significance (p = 0.07). Linear regression analysis between mutation efficiency and Sox2 expression revealed no significant correlation for either stage 20, 30, or both stages combined (**Figure 9B, D, F**).

RT-qPCR expression analysis for tubb2b is summarized in **Table 2** and **Figure 10**. There was a significant difference in *Tubb2b* expression at stage 30 between HALF and non-injected control embryos (p = 0.02) at stage 30. There was no other significant difference for tubb2b

Summary of Sox2 qPCR Expression						
Both Stages						
Condition	**Average Fold Change**	**Standard Deviation**	**No. of Embryos**	**Vs. CON P-value**	**Vs. FLDX P-value**	**Vs. 1.15 P-value**
FULL	2.63	4.10	16	0.50	0.17	0.04*
HALF	0.20	0.20	2	0.14	0.46	
FLDX	0.79	1.18	4	0.20		
Control	4.68	8.31	10			
Stage 20						
FULL	0.17	0.24	4	0.41		
Control	4.7	6.13	3			
Stage 30						
FULL	4.70	6.23	12	0.54	0.24	0.04*
HALF	0.28	0.28	2	0.07	0.44	
FLDX	1.47	1.75	3	0.36		
Control	3.26	3.49	7			

Table 1. Summary of Sox2 qPCR Expression.
FULL (2.3ng gRNA , 5.2ng Cas9); HALF (1.15ng gRNA, 2.6ng Cas9); FLDX (5% Fluoresceinated lysine-fixable dextran); Control (non-injected controls) (*= $p \leq 0.05$, ** = $p \leq 0.01$; *** = $p \leq 0.001$)

expression, although the difference between non-injected controls and FULL ($p = 0.12$) and FLDX ($p = 0.09$) were just over the cut off for significance. There was no significant correlation between mutation efficiency and *Tubb2b* expression at either stage 20 or 30 combined or separately, (**Figure 10 B, D, F**). The correlation between mutation efficiency and tubb2b expression at stage 30 was just over the cut off for significance ($R^2 = 0.14$, $p = 0.10$, $n = 20$) **(Figure 10F**).

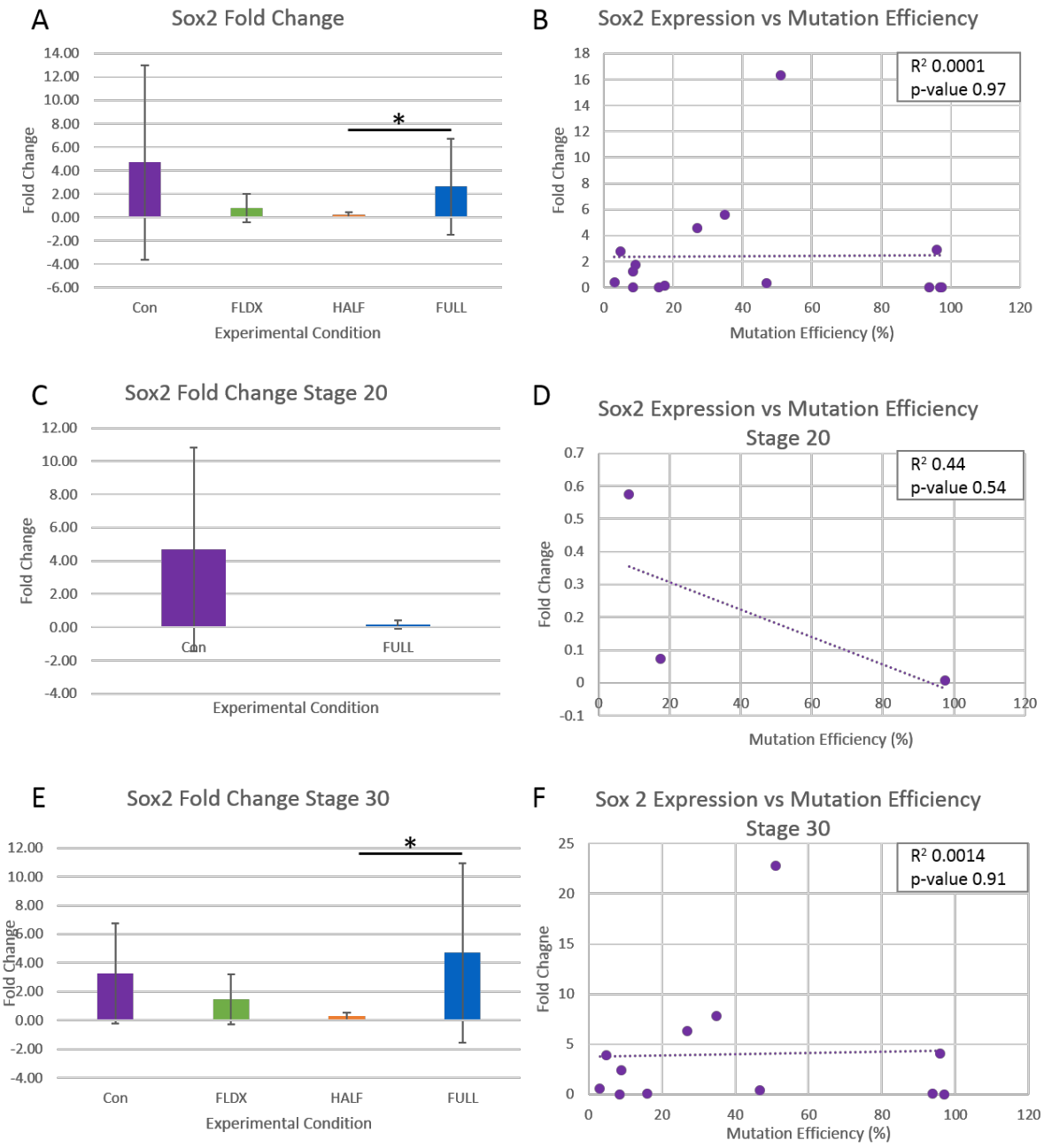

Figure 9. Sox2 Expression in Ttyh1 Knockouts.

Expression of Sox2 via RT-qPCR. (A) Fold Change of FULL (n =16), HALF (n = 2), FLDX (n =4), and Con (n =10) stages 20 and 30 combined. (B) Fold change compared to TIDE analysis mutation efficiency in FULL and HALF (n = 15) embryos of stages 20 and 30, R^2 of linear regression analysis and p-value of fit. (C) Fold Change of FULL (n = 4) and Con (n =3) at stage 20. (D) Fold change compared to TIDE analysis mutation efficiency in FULL and HALF (n = 3) at stage 30 and R^2 of linear regression analysis and p-value of fit. (E) Fold Change of FULL (n =12), HALF (n = 2), FLDX (n = 3), and Con (n = 7) at stage 30. (F) Fold change compared to TIDE analysis mutation efficiency in FULL and HALF (n = 12) R^2 of linear regression analysis and p-value of fit (* = $p \leq 0.05$; ** = $p \leq 0.01$; *** = $p \leq 0.001$), error bars indicate 1 standard deviation.

Summary of tubb2b qPCR Expression						
Both Stages						
Condition	**Average Fold Change**	**Standard Deviation**	**No. of Embryos**	**Vs. CON P-value**	**Vs. FLDX P-value**	**Vs. 1.15 P-value**
FULL	1.78	2.52	29	0.32	0.17	0.30
HALF	2.55	1.55	9	0.44	0.43	
FLDX	3.55	2.37	6	0.65		
Control	5.05	11.66	15			
Stage 20						
FULL	0.41	0.37	10	0.23	0.19	0.47
HALF	0.69	0.58	3	0.27	0.85	
FLDX	0.60	0.05	2	0.26		
Control	3.51	5.09	6			
Stage 30						
FULL	4.45	6.47	19	0.12	0.22	0.57
HALF	5.94	2.92	6	0.02*	0.36	
FLDX	9.55	5.56	4	0.09		
Control	1.81	1.76	7			

Table 2. Summary of Tubb2b qPCR Expression
FULL (2.3ng gRNA , 5.2ng Cas9); HALF (1.15ng gRNA, 2.6ng Cas9); FLDX (5% Fluoresceinated lysine-fixable dextran); Control (non-injected controls) (*= $p \leq 0.05$, ** = $p \leq 0.01$; *** = $p \leq 0.001$)

The summary of Notch1 expression can be found in **Table 3** and **Figure 11.** There was a significant difference between the non-injected controls and the FLDX injected controls ($p = 0.03$). There was no significant difference between any of the other experimental conditions, however the difference between non-injected controls and HALF fell just under significant ($p = 0.08$) at stage 30 and both conditions combined, as did the difference between FULL and HALF

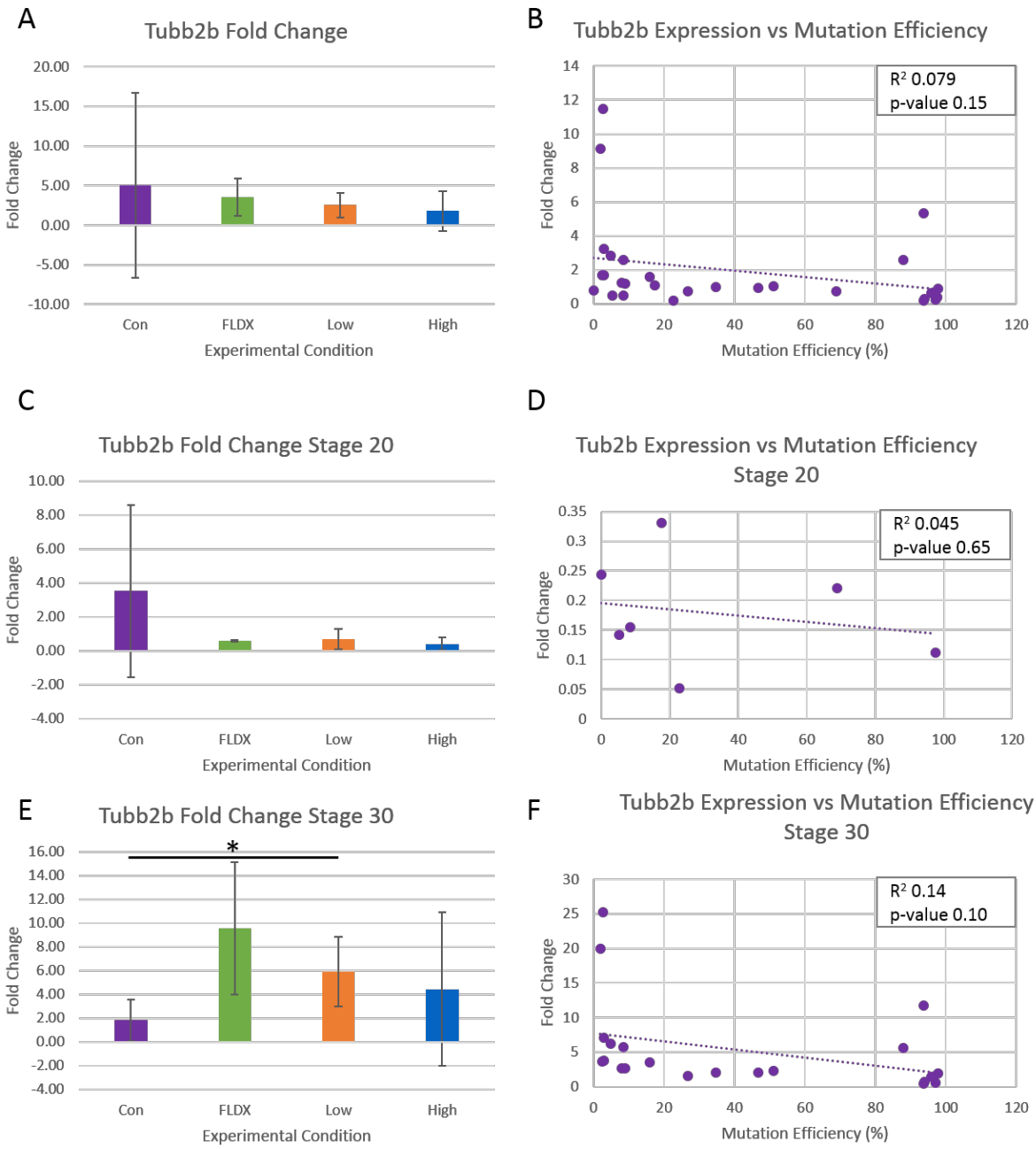

Figure 10. Tubb2b Expression in Ttyh1 Knockouts.
Expression of *Tubb2b* via RT-qPCR. (A) Fold Change of FULL (n =29), HALF (n = 9), FLDX (n =6), and Con (n =15) stages 20 and 30 combined. (B) Fold change compared to TIDE analysis mutation efficiency in FULL and HALF (n = 23) embryos of stages 20 and 30, R^2 of linear regression analysis and p-value of fit. (C) Fold Change of FULL (n = 10), HALF (n = 3), FLDX (n =2) and Con (n =6) at stage 20. (D) Fold change compared to TIDE analysis mutation efficiency in FULL and HALF (n = 7) at stage 30 and R^2 of linear regression analysis and p-value of fit. (E) Fold Change of FULL (n =19), HALF (n = 6), FLDX (n = 4), and Con (n = 7) at stage 30. (F) Fold change compared to TIDE analysis mutation efficiency in FULL and HALF (n = 21) R^2 of linear regression analysis and p-value of fit (* = $p \leq 0.05$; ** = $p \leq 0.01$; *** = $p \leq 0.001$), error bars indicate 1 standard deviation.

Summary of Notch1 qPCR Expression						
Both Stages						
Condition	**Average Fold Change**	**Standard Deviation**	**No. of Embryos**	**Vs. CON P-value**	**Vs. FLDX P-value**	**Vs. 1.15 P-value**
FULL	1.27	1.50	28	0.83	0.49	0.14
HALF	0.76	0.45	8	0.08	0.42	
FLDX	4.07	7.32	5	0.50		
Control	1.36	1.03	15			
Stage 20						
FULL	2.11	2.45	10	0.63		0.26
HALF	0.98	0.71	3	0.46		
Control	1.61	1.38	6			
Stage 30						
FULL	0.84	0.39	18	0.23	0.06	0.15
HALF	0.64	0.18	5	0.08	0.25	
FLDX	0.39	0.29	4	0.03*		
Control	1.21	0.82	9			

Table 3. Summary of Notch1 qPCR Expression.
FULL (2.3ng gRNA , 5.2ng Cas9); HALF (1.15ng gRNA, 2.6ng Cas9); FLDX (5% Fluoresceinated lysine-fixable dextran); Control (non-injected controls) (*= $p \leq 0.05$, ** = $p \leq 0.01$; *** = $p \leq 0.001$)

at stage 30 ($p = 0.06$). There was no significant relationship between Notch1 expression and mutation efficiency for either stage separately, or for the two stages combined (**Figure 11B, D, F**).

Expression analysis for Ttyh2 is summarized in **Table 4** and **Figure 12**. There was no significant relationship between any of the experimental conditions at any stage separately or

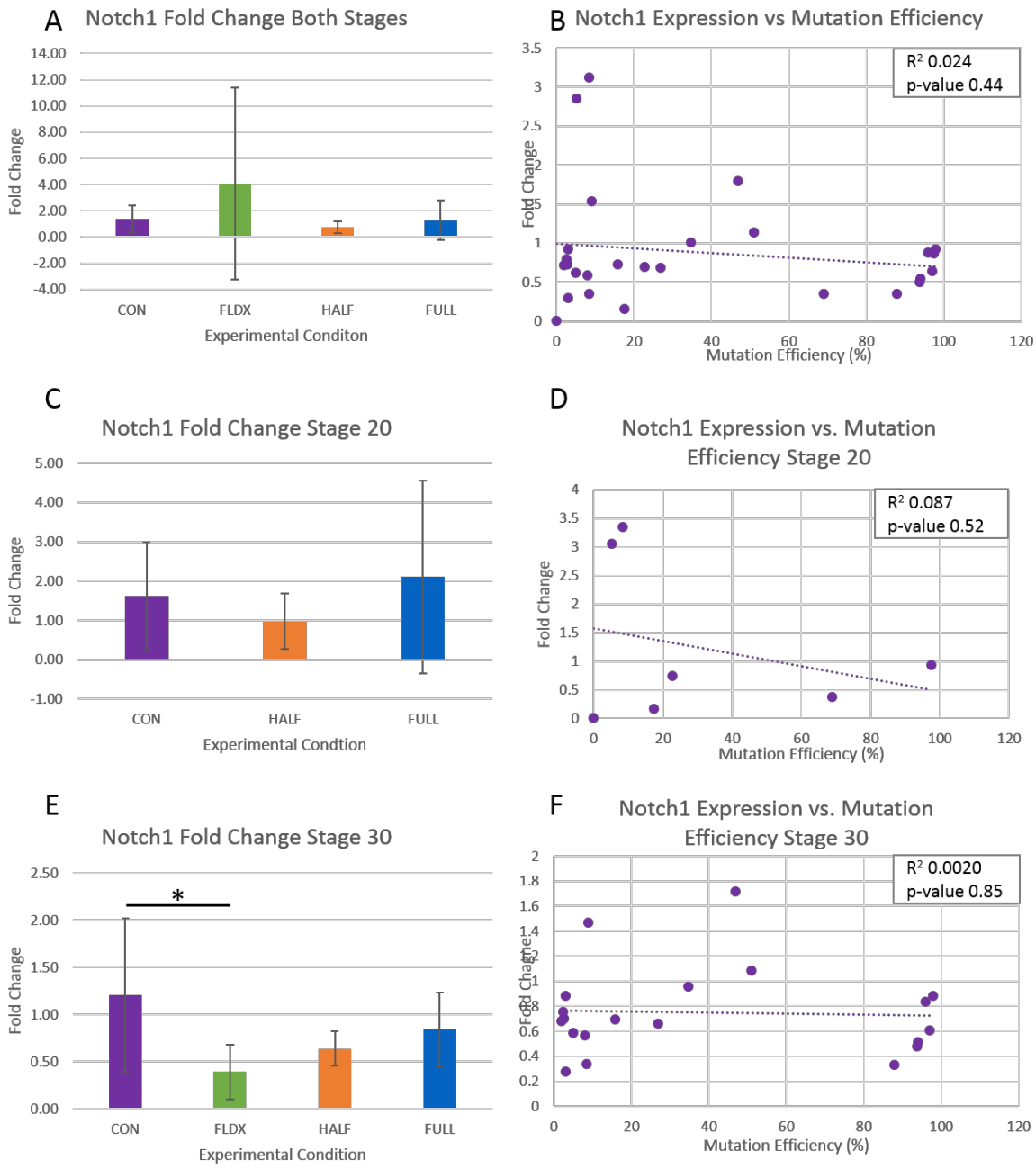

Figure 11. Notch1 Expression in Ttyh1 Knockouts.
Expression of Sox2 via RT-qPCR. (A) Fold Change of FULL (n =28), HALF (n = 8), FLDX (n = 5), and Con (n = 15) stages 20 and 30 combined. (B) Fold change compared to TIDE analysis mutation efficiency in FULL and HALF (n = 27) embryos of stages 20 and 30, R^2 of linear regression analysis and p-value of fit. (C) Fold Change of FULL (n = 10), HALF (n = 3) and Con (n =6) at stage 20. (D) Fold change compared to TIDE analysis mutation efficiency in FULL and HALF (n = 7) at stage 30 and R^2 of linear regression analysis and p-value of fit. (E) Fold Change of FULL (n = 18), HALF (n = 5), FLDX (n = 4), and Con (n = 9) at stage 30. (F) Fold change compared to TIDE analysis mutation efficiency in FULL and HALF (n = 20) R^2 of linear regression analysis and p-value of fit (* = $p \leq 0.05$; ** = $p \leq 0.01$; *** = $p \leq 0.001$), error bars indicate 1 standard deviation.

Summary of Ttyh2 qPCR Expression						
Both Stages						
Condition	**Average Fold Change**	**Standard Deviation**	**No. of Embryos**	**Vs. CON P-value**	**Vs. FLDX P-value**	**Vs. 1.15 P-value**
FULL	1.85	2.01	28	0.25	0.94	0.21
HALF	1.17	0.98	8	0.81	0.54	
FLDX	1.93	2.21	5	0.60		
Control	1.29	1.17	15			
Stage 20						
FULL	2.44	2.50	10	0.41		0.25
HALF	1.13	0.94	3	0.71		
Control	1.51	1.58	6			
Stage 30						
FULL	1.49	1.39	18	0.34	0.19	0.64
HALF	1.20	1.01	5	0.89	0.62	
FLDX	0.89	0.48	4	0.52		
Control	1.12	0.56	9			

Table 4. Summary of Ttyh2 qPCR Expression.
FULL (2.3ng gRNA , 5.2ng Cas9); HALF (1.15ng gRNA, 2.6ng Cas9); FLDX (5% Fluoresceinated lysine-fixable dextran); Control (non-injected controls) (*= $p \leq 0.05$, ** = $p \leq 0.01$; *** = $p \leq 0.001$)

combined. There was also no correlation between mutation efficiency and Ttyh2 expression for either stage combined or separately (**Figure 12B, D, F**).

Expression analysis for Ttyh3 is summarized in **Table 5** and **Figure 13**. There was a significant difference between FULL embryos and FLDX at stage 30 (P = 0.01) and at both stage combined (p = 0.01). There was a significant difference between FLDX and the non-injected control embryos at stage 30 (p = 0.02) and at both stages combined (p = 0.03). In addition,

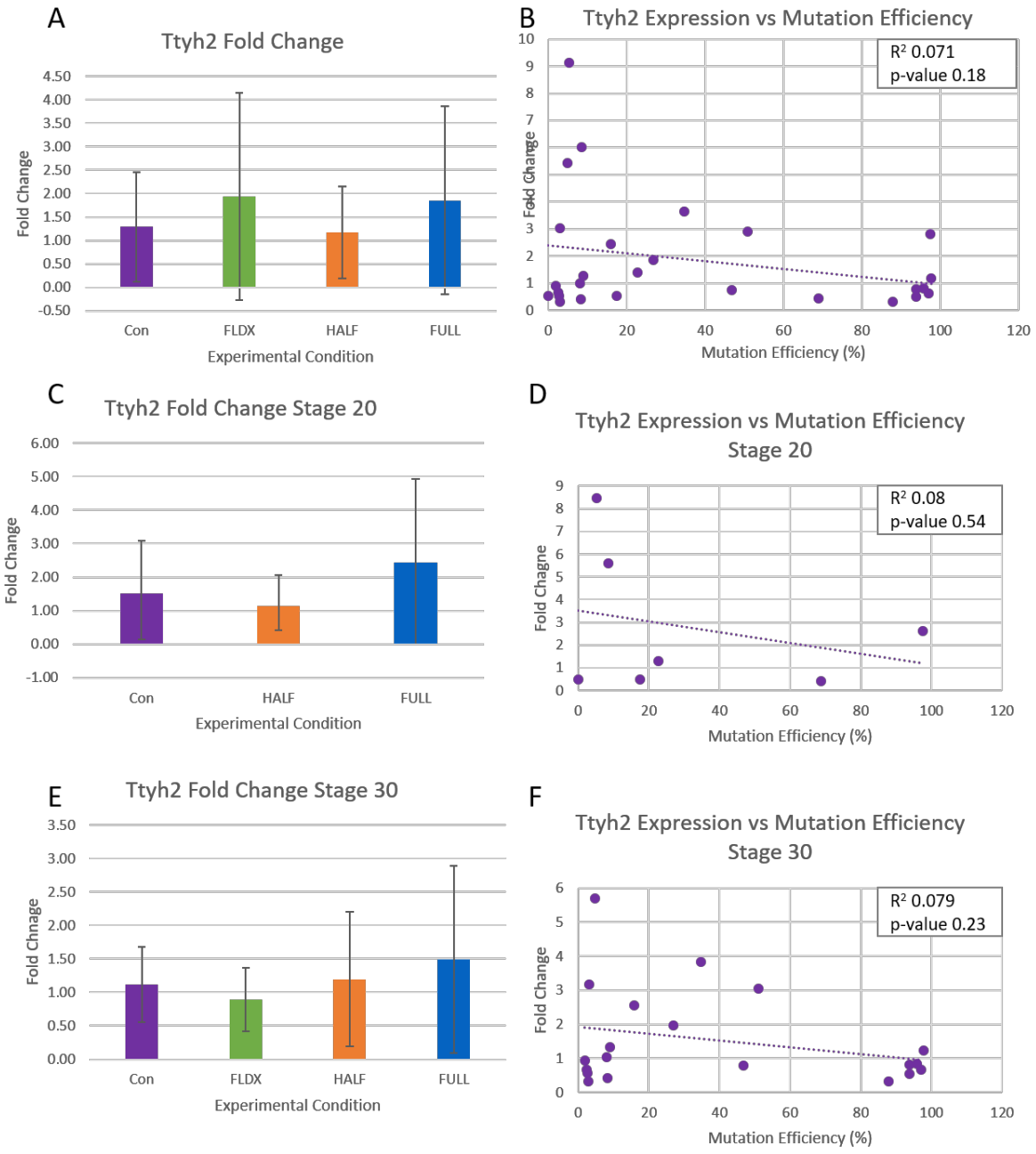

Figure 12. Ttyh2 Expression in Ttyh1 Knockouts.

Expression of *Ttyh2* via RT-qPCR. (A) Fold Change of FULL (n =28), HALF (n = 8), FLDX (n = 5), and Con (n = 15) stages 20 and 30 combined. (B) Fold change compared to TIDE analysis mutation efficiency in FULL and HALF (n = 27) embryos of stages 20 and 30, R^2 of linear regression analysis and p-value of fit. (C) Fold Change of FULL (n = 10), HALF (n = 3) and Con (n =6) at stage 20. (D) Fold change compared to TIDE analysis mutation efficiency in FULL and HALF (n = 7) at stage 30 and R^2 of linear regression analysis and p-value of fit. (E) Fold Change of FULL (n = 18), HALF (n = 5), FLDX (n = 4), and Con (n = 9) at stage 30. (F) Fold change compared to TIDE analysis mutation efficiency in FULL and HALF (n = 20) R^2 of linear regression analysis and p-value of fit (* = $p \leq 0.05$; ** = $p \leq 0.01$; *** = $p \leq 0.001$), error bars indicate 1 standard deviation.

Summary of Ttyh3 qPCR Expression						
Both Stages						
Condition	**Average Fold Change**	**Standard Deviation**	**No. of Embryos**	**Vs. CON P-value**	**Vs. FLDX P-value**	**Vs. 1.15 P-value**
FULL	1.28	0.86	25	0.68	0.01**	0.15
HALF	0.83	0.64	8	0.17	0.30	
FLDX	0.52	0.28	4	0.03*		
Control	1.45	1.28	13			
Stage 20						
FULL	1.87	1.62	9	0.28		0.85
HALF	1.58	1.73	3	0.75		
Control	1.13	0.59	5			
Stage 30						
FULL	0.98	0.55	16	0.36	0.01**	0.04*
HALF	0.55	0.25	5	0.09	0.26	
FLDX	0.32	0.20	3	0.02*		
Control	1.34	0.99	8			

Table 5. Summary of Ttyh3 qPCR Expression.
FULL (2.3ng gRNA, 5.2ng Cas9); HALF (1.15ng gRNA, 2.6ng Cas9); FLDX (5% Fluoresceinated lysine-fixable dextran); Control (non-injected controls) (*= $p \leq 0.05$, ** = $p \leq 0.01$; *** = $p \leq 0.001$)

there was significant differenced between FULL and HALF embryos at stage 30 ($p = 0.04$). There was no correlation between *Ttyh3* expression and mutation efficiency for any stage separately or combined (**Figure13B, D, F**).

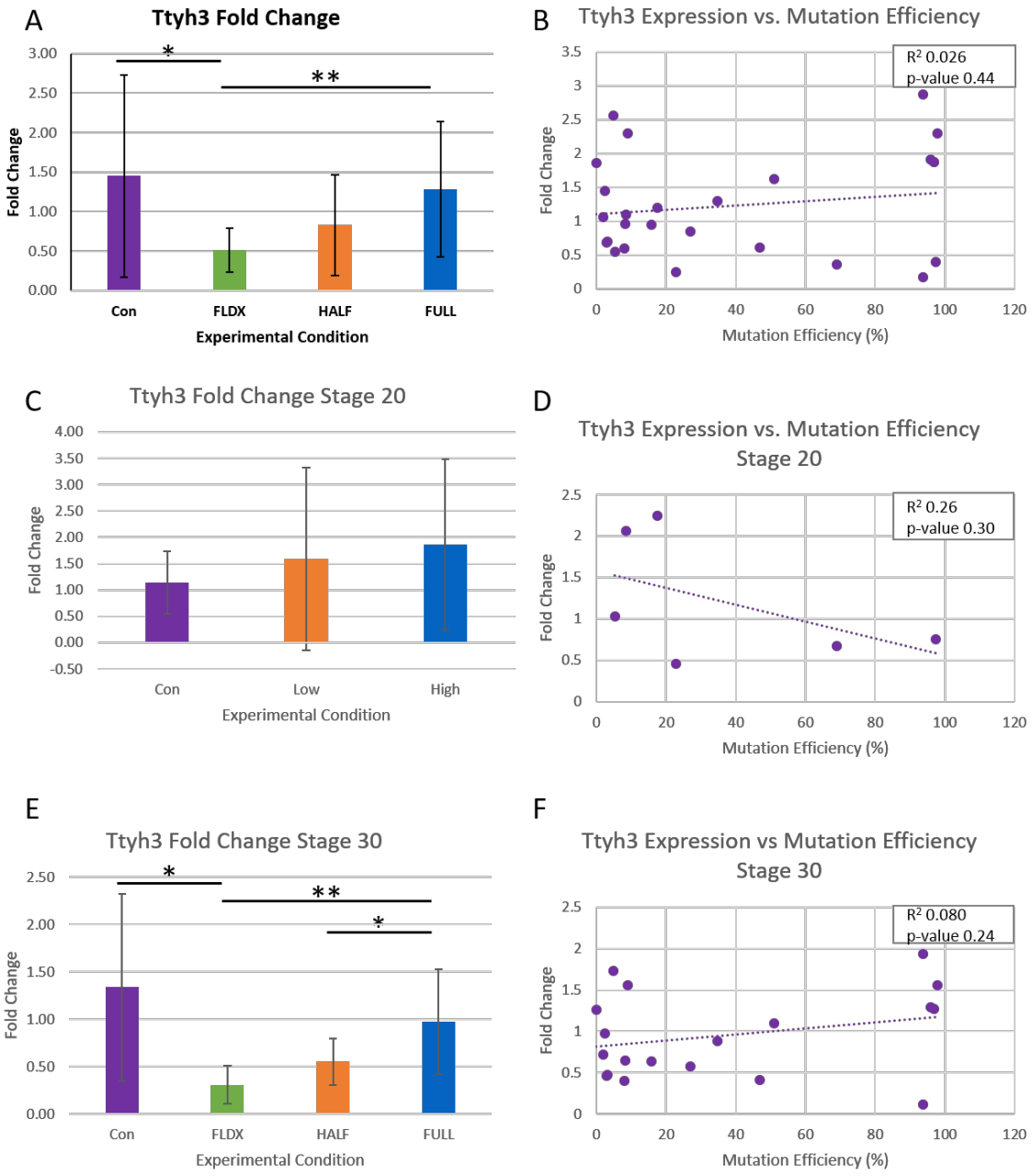

Figure 13. Ttyh3 Expression in Ttyh1 Knockouts.

Expression of *Ttyh3* via RT-qPCR. (A) Fold Change of FULL (n =25), HALF (n = 8), FLDX (n = 4), and Con (n = 13) stages 20 and 30 combined. (B) Fold change compared to TIDE analysis mutation efficiency in FULL and HALF (n = 25) embryos of stages 20 and 30, R^2 of linear regression analysis and p-value of fit. (C) Fold Change of FULL (n = 9), HALF (n = 3) and Con (n =5) at stage 20. (D) Fold change compared to TIDE analysis mutation efficiency in FULL and HALF (n = 6) at stage 30 and R^2 of linear regression analysis and p-value of fit. (E) Fold Change of FULL (n = 16), HALF (n = 5), FLDX (n = 3), and Con (n = 8) at stage 30. (F) Fold change compared to TIDE analysis mutation efficiency in FULL and HALF (n = 19) R^2 of linear regression analysis and p-value of fit (* = $p \leq 0.05$; ** = $p \leq 0.01$; *** = $p \leq 0.001$), error bars indicate 1 standard deviation.

Discussion

Analysis of mutation efficiency via TIDE showed that injection of gene specific gRNA and Cas9 bilaterally at the 2-cell stage is able to induce an insertion or deletion (INDEL) mutation in *Xenopus laevis* embryos with an average mutation efficiency of 41.4%. In addition, injection of the higher concentration was able to induce a higher mutation efficiency although there was a large variation in both HALF and FULL embryos. This is comparable to other CRISPR/Cas9 indel frequencies ranging from an average of 17.7% to 83.3% in *Xenopus laevis* and *X. tropicalis*, a closely related species (Gagon et al., 2014; Banach et al., 2016; Guo et al., 2014; Wang et al., 2015).

Variation in the mutation efficiency could be due to unsuccessful delivery of the construct, or degradation before the construct is able to induce a mutation. To increase the mutation efficiency, future experiments could inject higher concentrations of gRNA and Cas9 or investigate modified delivery methods to protect the construct from degradation (Feehan et al., 2017; Guo et al., 2014). Low efficiencies and high variation could also be due to the purity of gDNA used for TIDE analysis. The TIDE program utilizes the chromatogram that accompanies Sanger sequencing, which normally is an indication of sequence purity, to analyze the variation in the control and test sequence (Brinkman et al., 2014). To extract gDNA and mRNA from the same sample simultaneously Fisher TRI reagent was used. TRI reagent provided good purity and subsequent reverse transcription of mRNA, but resulted in poor quality and low yield of gDNA making subsequent PCR and sequencing more challenging. Implementation of another reagent for mRNA and gDNA extractions may increase the purity and yield of gDNA. Thus, increasing the purity of the gDNA may help to reduce noise and improve accuracy of the calculated mutation

efficiency. Another approach to increasing mutation efficiency would be to utilize CRISPR/Cas9 knockin technology to insert a stop codon in the gene of interest to assure the induced mutation results in a non-functional protein (Gagnon et al., 2014).

Consistent with the literature mutation efficiency increased as the embryo developed, although the degree of difference was not statistically significant (Bhattacharya et al., 2015). Analysis of mutation efficiency at a later stage may help to verify this trend.

Investigation of mortality resulted in increased mortality for all injected experimental conditions as compared to the control. This would imply that the increased mortality is due to the injection procedure as opposed to knockout of*Ttyh1*. This is in contrast with Kumada et al., 2010, who provided evidence that double knockout of*Ttyh1* in mice was embryonically lethal during neural development. This is consistent with earlier findings that partial removal of *ttyh1,* the Drosophila homeolog, along with *flightless* was not lethal (Campbell et al., 1993). One possible explanation for the lack of lethality is that *Xenopus laevis* is a pseudo-tetraploid organism and the gRNA was designed to have a higher affinity for the "long" copy of *Ttyh1*. In addition, the primers were designed for the "long" copy so PCR and subsequent sequencing analysis likely did not include the "short" copy in determination of mutation efficiency. Thus, it is possible that the short copy provides some protective compensation that maintains viability. Future investigations with both homeolog specific gRNA may induce higher mortality and a more severe phenotype. There was also a high degree of variability in the survival percentage of FULL and FLDX embryos and additional mortality experiments should be conducted to potentially reduce the variation observed between replicates. In addition, increasing mutation efficiencies could also lead to a more severe phenotype.

Sox2 expression was more intense in*Ttyh1* knockouts in whole mount embryos and histology most evidently at stage 30, which is when*Ttyh1* peaks in expression in *Xenopus laevis* (Sessions et al., 2016. By stage 40 there was still a slight difference between bilaterally injected embryos and control embryos, however differences were less noticeable in unilaterally injected stage 40 embryos. RT-qPCR indicated a significant difference between FULL and HALF at stage 30, while all other comparisons between different experimental conditions did not reveal significant differences. In addition, there was not a significant correlation between mutation efficiency and *Sox2* expression. However, out of all the genes tested via qPCR, *Sox2* had the lowest *n* and the most difficulty with the probe. To confirm qPCR data, further examination of *Sox2* should be done with a new probe to assess whether the inability to detect is due to a faulty probe or low expression of *Sox2*. If further investigation is consistent with *in situ* data this would suggest that knockout of *Ttyh1* reduces expression of *Sox2*. As *Sox2* encodes a transcription factor that maintains neural progenitor identity and acts as a marker for neural progenitor cells, this decreased expression could be due to either a reduction in cell number or increased differentiation (Graham et al., 2003). DAPI staining and cell counts on histological sections of unilaterally injected embryos could be done to determine if *Ttyh1* knockouts affects cell count. However, as *Ttyh1* overexpression has been implicated in maintenance of stem cell capacity, confirmed reduction of *Sox2* expression in *Ttyh1* knockouts would suggest that *Ttyh1* plays a role in maintenance of neural progenitor cells (Kim et al., 2018).

Analysis of *tubb2b* expression revealed a higher expression in the injected side of unilateral *Ttyh1* knockout embryos at stage 20, while stage 30 and 40 had lower expression on the injected side. RT-qPCR expression analysis resulted in significantly higher expression of

Tubb2b HALF embryos compared to controls at stage 30. However, there was no correlation between mutation efficiency and *Tubb2b* expression. The lack of significant results for qPCR expression analysis could be due to differences in expression requiring greater spatial resolution. For example, in unilaterally injected embryos at stage 30 there was clear difference in the neural crest, but expression was more similar in the eye regions, and more intense in the prosencephalon of the injected side. To gain more quantitative analysis of *in situ* expression, image analysis of histological sections could be performed. In addition, to increase the accuracy of the RT-qPCR analysis, it may help to isolate the neural tissue to as the genes of interest are localized to the nervous system.

If further investigation is able to determine that *Ttyh1* knockout increases *tubb2b* expression and reduces *Sox2* expression this would support that *Ttyh1* has a role in the maintenance of neural progenitor cells and that lack of *Ttyh1* promotes neural differentiation. Alternatively, *tubb2b* is a neural specific tubulin and *Ttyh1* is known to interact with cytoskeletal proteins such as actin filaments in filopodia and tumor microtubes, as well as promote neurite-like projections (Mathews et al., 2007; Jung et al., 2017; Stefaniuk et al., 2010a). Thus, to confirm whether *Ttyh1* knockouts are affecting neural differentiation or cytoskeletal and axonal development via *tubb2b,* future studies should corroborate the increase of differentiated neurons using another neural cell marker. If Ttyh1 is more specifically affecting the cytoskeleton components, investigations into cellular morphology of *Ttyh1* knockouts, such as other tubulin genes would be beneficial.

Notch1 expression analysis resulted in no significant difference between experimental conditions at either of the analyzed stages. There was also no correlation between *Notch1*

expression and mutation efficiency. This is consistent within the literature that *Ttyh1* overexpression does not affect expression of Notch on the mRNA or protein level but rather changes the amount of ICD in the cell (Kim et al., 2018). To confirm this, future investigations should investigate how *Ttyh1* knockout affect the levels of endogenous ICD and other downstream genes of the Notch signaling pathway.

Analysis of *Ttyh2* in *Ttyh1* knockouts did not display any significant difference in either stage or any of the experimental conditions. Nor was there a correlation between expression and mutation efficiency. Thus, it is unlikely that *Ttyh2* is acting in a compensatory manner. This is in accordance with the literature, as *Ttyh2* differs in expression patterns from *Ttyh1,* coming on later at hatching stages, 34-35, as opposed to early blastula stages, 19-20 (Halleran et al., 2015). In addition, *Ttyh2* is known to be Calcium dependent, whereas *Ttyh1* has a calcium binding site, but is volume activated (Suzuki et al., 2004).

Ttyh3 expression did show significant increase in expression in FULL *Ttyh1* knockout embryos as compared to FLDX and HALF embryos at stage 30. *Ttyh1* and *Ttyh3* both begin to be detected at neurula stages with strong localization to the anterior nervous system (Halleran et al., 2015). However, by swimming tadpole stages, 35-37, their expression becomes mutually exclusive with *Ttyh1* localizing to ventricular mitotic zones, whereas *Ttyh3* localized to post-mitotic zones (Halleran et al., 2015). In addition, *Ttyh3,* as a calcium dependent channel, is known to have a greater homology to *Ttyh2* (Suzuki et al., 2004). Thus, the increase of *Ttyh3* in *Ttyh1* knockouts may not be compensatory. The increased expression could be evidence of an increase in post-mitotic neurons, supporting the notion *Ttyh1* plays a role in the maintenance of mitotic neurons. To confirm this, spatial gene expression analysis of *Ttyh3* should be

conducted to determine if *Ttyh1* knockout results in differential spatial expression of *Ttyh3.* Spatial analysis may reveal that *Ttyh3* encroaches on mitotic regions in the absence of *Ttyh1*. In addition, to confirm that such encroachment is due to a decrease in mitotic cell population, expression analysis of mitotic and post-mitotic cell markers should be conducted in *Ttyh1* knockouts.

One limitation of the qPCR data is that RNA was extracted from whole embryos. All of the genes investigated in this study have high localization to the nervous system and perhaps inclusion of other tissues decreased the ability of the probes to detect the gene of interest and may have contributed to the high degree of variation observed in many of the samples. To correct for this, neural tissues could be isolated prior to RNA extraction and analysis. In addition, qPCR was only performed on stage 20 and 30 embryos, expanding analysis to stage 40 may also provide further insight into the effects of *Ttyh1* knockout, as expression of *Ttyh1* is relatively stable by late tailbud stages (Session et al., 2016; Halleran et al., 2015)

Conclusion

In summary CRISPR/Cas9 was able to successfully induce knockouts of *Ttyh1* in *Xenopus laevis*. Knockout of *Ttyh1* did not have significant effects on embryo survival as compared to FLDX injected controls. *In situ* hybridization of *Ttyh1* knockout embryos revealed differential expression of *Sox2* and *tubb2b*. *Sox2* expression was lower in *Ttyh1* knockouts at stages 30, hatching stages, and stage 40, tailbud stages. *Tubb2b* expression was higher at stage 20, neurula stages, but lower at stage 30, hatching stages, and stage 40, tailbud stages. qPCR analysis of Sox2 expression was significantly higher in FULL compared to HALF embryos at stage

30, but was not significant between any other condition. There was no correlation between mutation efficiency and *Sox2* expression. *Tubb2b* qPCR expression was significantly higher in HALF embryos as compared to non-injected controls. There was no significant difference in *tubb2b* expression at any other stage, nor was there a correlation between mutation efficiency and *tubb2b* expression. qPCR analysis resulted in a significant increase of *Notch1* expression of non-injected controls as compared to FLDX embryos. There was no significant relationship between *Notch1* expression and *Ttyh1* mutation efficiency. Analysis of Ttyh2 expression revealed no significant difference between and of the experimental conditions, nor was there a correlation between mutation efficiency and *Ttyh2* expression. *Ttyh3* qPCR analysis revealed a significant increase in *Ttyh3* expression in FULL embryos as compared to HALF embryos and FLDX injected controls. There was also a significant decrease in *Ttyh3* expression in FLDX as compared to non-injected controls. There was no correlation between mutation efficiency and *Ttyh3* expression. These results suggest that the Ttyh1 gene may play a role in maintenance of neural progenitor cells but does not do so through the expression of Notch1. In addition, Ttyh2 does not appear to compensate for knockout of *Ttyh1*. *Ttyh3* expression may expand due to knockout of *Ttyh1*, but it is unclear if it is acting in a compensatory manner. Thus, we concluded that that Ttyh1 has a role in neurodevelopment, but further investigation is required to determine its specific effect.

References

Banach, M., Edholm, E., & Robert, J. (2017). Exploring the functions of nonclassical MHC class ib genes in xenopus laevis by the CRISPR/Cas9 system. *Developmental Biology, 426*(2), 261-269.

Bhattacharya, D., Marfo, C. A., Li, D., Lane, M., & Khokha, M. K. (2015). CRISPR/Cas9: An inexpensive, efficient loss of function tool to screen human disease genes in xenopus. *Developmental Biology, 408*(2), 196-204.

Bolós, V., Grego-Bessa, J., & de la Pompa, José Luis. (2007). Notch signaling in development and cancer. *Endocrine Reviews, 28*(3), 339-363.

Brinkman, E. K., Chen, T., Amendola, M., & van Steensel, B. (2014). Easy quantitative assessment of genome editing by sequence trace decomposition. *Nucleic Acids Research, 42*(22), e168-e168.

Campbell, H. D., Kamei, M., Claudianos, C., Woollatt, E., Sutherland, G. R., Suzuki, Y., . . . Young, I. G. (2000). Human and mouse homologues of the drosophila melanogaster tweety (tty) gene: A novel gene family encoding predicted transmembrane proteins. *Genomics, 68*(1), 89-92.

Campbell, H. D., Schimansky, T., Claudianos, C., Ozsarac, N., Kasprzak, A. B., Cotsell, J. N., . . . Miklos, G. L. (1993). The drosophila melanogaster flightless-I gene involved in gastrulation and muscle degeneration encodes gelsolin-like and leucine-rich repeat domains and is conserved in caenorhabditis elegans and humans. *Proceedings of the National Academy of Sciences of the United States of America, 90*(23), 11386-11390.

Darweesh, A. S., Louka, M. L., Hana, M., Rashad, S., El-Shinawi, M., Sharaf-Eldin, A., & Kassim, S. K. (2014). Validation of analytical breast cancer microarray analysis in medical laboratory. *Medical Oncology, 31*(10), 201.

Gagnon, J. A., Valen, E., Thyme, S. B., Huang, P., Ahkmetova, L., Pauli, A., . . . Schier, A. F. (2014). Efficient mutagenesis by Cas9 protein-mediated oligonucleotide insertion and large-scale assessment of single-guide RNAs. *PloS One, 9*(5), e98186.

Graham, V., Khudyakov, J., Ellis, P., & Pevny, L. (2003). SOX2 functions to maintain neural progenitor identity. *Neuron, 39*(5), 749-765.

Guo, X., Zhang, T., Hu, Z., Zhang, Y., Shi, Z., Wang, Q., . . . Chen, Y. (2014). Efficient RNA/Cas9-mediated genome editing in xenopus tropicalis. *Development (Cambridge, England), 141*(3), 707-714. doi:10.1242/dev.099853 [doi]

Halleran, A. D., Sehdev, M., Rabe, B. A., Huyck, R. W., Williams, C. C., & Saha, M. S. (2014). Characterization of tweety gene (ttyh1-3) expression in xenopus laevis during embryonic development. *Gene Expression Patterns : GEP, 17*(1), 38-44. doi:10.1016/j.gep.2014.12.002

Hausen, P., & Riebesell, M. (1991). *The early development of xenopus laevis: An atlas of the histology* Verlag Der Zeitschrift F'Ur Naturforschung.

He, Y., Hryciw, D. H., Carroll, M. L., Myers, S. A., Whitbread, A. K., Kumar, S., . . . Hooper, J. D. (2008). The ubiquitin-protein ligase Nedd4-2 differentially interacts with and regulates members of the tweety family of chloride ion channels. *The Journal of Biological Chemistry, 283*(35), 24000-24010. doi:10.1074/jbc.M803361200 [doi]

Huyck, R. W., Nagarkar, M., Olsen, N., Clamons, S. E., & Saha, M. S. (2015). Methylmercury exposure during early xenopus laevis development affects cell proliferation and death but not neural progenitor specification. *Neurotoxicology and Teratology, 47*, 102-113.

Jung, E., Osswald, M., Blaes, J., Wiestler, B., Sahm, F., Schmenger, T., . . . Winkler, F. (2017). Tweety-homolog 1 drives brain colonization of gliomas. *The Journal of Neuroscience : The Official Journal of the Society for Neuroscience, 37*(29), 6837-6850. doi:10.1523/JNEUROSCI.3532-16.2017 [doi]

Kim, J., Han, D., Byun, S. H., Kwon, M., Cho, J. Y., Pleasure, S. J., & Yoon, K. (2018). Ttyh1 regulates embryonic neural stem cell properties by enhancing the notch signaling pathway. *EMBO Reports, 19*(11), 10.15252/embr.201745472. Epub 2018 Sep 3. doi:e45472 [pii]

Klein, S. L., Strausberg, R. L., Wagner, L., Pontius, J., Clifton, S. W., & Richardson, P. (2002). Genetic and genomic tools for xenopus research: The NIH xenopus initiative: A peer reviewed forum. *Developmental Dynamics: An Official Publication of the American Association of Anatomists, 225*(4), 384-391.

Kleinman, C. L., Gerges, N., Papillon-Cavanagh, S., Sin-Chan, P., Pramatarova, A., Quang, D. K., . . . Djambazian, H. (2014). Fusion of TTYH1 with the C19MC microRNA cluster drives expression of a brain-specific DNMT3B isoform in the embryonal brain tumor ETMR. *Nature Genetics, 46*(1), 39.

Kopan, R., & Ilagan, M. X. G. (2009). The canonical notch signaling pathway: Unfolding the activation mechanism. *Cell, 137*(2), 216-233.

Kumada, T., Yamanaka, Y., Kitano, A., Shibata, M., Awaya, T., Kato, T., . . . Nakahata, T. (2010). Ttyh1, a Ca2 -binding protein localized to the endoplasmic reticulum, is required for early embryonic development. *Developmental Dynamics, 239*(8), 2233-2245.

Matthews, C. A., Shaw, J. E., Hooper, J. A., Young, I. G., Crouch, M. F., & Campbell, H. D. (2007). Expression and evolution of the mammalian brain gene Ttyh1. *Journal of Neurochemistry, 100*(3), 693-707.

Moody, S. A., Miller, V., Spanos, A., & Frankfurter, A. (1996). Developmental expression of a neuron-specific β-tubulin in frog (xenopus laevis): A marker for growing axons during the embryonic period. *Journal of Comparative Neurology, 364*(2), 219-230.

Nakayama, T., Blitz, I. L., Fish, M. B., Odeleye, A. O., Manohar, S., Cho, K. W., & Grainger, R. M. (2014). Cas9-based genome editing in xenopus tropicalis. *Methods in enzymology* (pp. 355-375) Elsevier.

Nieuwkoop, P. D., & Faber, J. (1994). Normal table of. *Xenopus Laevis,* , 252.

Penton, A. L., Leonard, L. D., & Spinner, N. B. (2012). Notch signaling in human development and disease. Paper presented at the *Seminars in Cell & Developmental Biology, , 23*(4) 450-457.

Pownall, M. (2018). Compensatory responses to Notch signaling perturbation in polyploid vertebrates, Xenopus laevis and Xenopus borealis, during embryonic development. *Unpublished Honors Thesis.*

Session, A. M., Uno, Y., Kwon, T., Chapman, J. A., Toyoda, A., Takahashi, S., . . . Kondo, M. (2016). Genome evolution in the allotetraploid frog xenopus laevis. *Nature, 538*(7625), 336.

Shimojo, H., Ohtsuka, T., & Kageyama, R. (2011). Dynamic expression of notch signaling genes in neural stem/progenitor cells. *Frontiers in Neuroscience, 5*, 78.

Siebel, C., & Lendahl, U. (2017). Notch signaling in development, tissue homeostasis, and disease. *Physiological Reviews, 97*(4), 1235-1294.

Sive, H. L., Grainger, R. M., & Harland, R. M. (2000). *Early development of xenopus laevis: A laboratory manual* CSHL Press.

Stefaniuk, M., & Lukasiuk, K. (2010). Cloning of expressed sequence tags (ESTs) representing putative epileptogenesis-related genes and the localization of their expression in the normal brain. *Neuroscience Letters, 482*(3), 230-234.

Stefaniuk, M., Swiech, L., Dzwonek, J., & Lukasiuk, K. (2010). Expression of Ttyh1, a member of the tweety family in neurons in vitro and in vivo and its potential role in brain pathology. *Journal of Neurochemistry, 115*(5), 1183-1194.

Suzuki, M., & Mizuno, A. (2004). A novel human cl(-) channel family related to drosophila flightless locus. *The Journal of Biological Chemistry, 279*(21), 22461-22468. doi:10.1074/jbc.M313813200 [doi]

Takebe, N., Nguyen, D., & Yang, S. X. (2014). Targeting notch signaling pathway in cancer: Clinical development advances and challenges. *Pharmacology & Therapeutics, 141*(2), 140-149.

Toiyama, Y., Mizoguchi, A., Kimura, K., Hiro, J., Inoue, Y., Tutumi, T., . . . Kusunoki, M. (2007). TTYH2, a human homologue of the drosophila melanogaster gene tweety, is up-regulated in colon

carcinoma and involved in cell proliferation and cell aggregation. *World Journal of Gastroenterology, 13*(19), 2717-2721.

Wang, F., Shi, Z., Cui, Y., Guo, X., Shi, Y., & Chen, Y. (2015). Targeted gene disruption in xenopus laevis using CRISPR/Cas9. *Cell & Bioscience, 5*(1), 15.

Wiernasz, E., Kaliszewska, A., Brutkowski, W., Bednarczyk, J., Gorniak, M., Kaza, B., & Lukasiuk, K. (2014). Ttyh1 protein is expressed in glia in vitro and shows elevated expression in activated astrocytes following status epilepticus. *Neurochemical Research, 39*(12), 2516-2526.